

Data Assimilation in a Wave Equation: A Variational Representer Approach for the Grenoble Tidal Model

F. H. Lyard

Proudman Oceanographic Laboratory, Bidston Observatory, Birkenhead, Merseyside L43 7RA, United Kingdom

Received January 14, 1997; revised February 27, 1998

We propose in this paper a synthesis of both the hydrodynamic and assimilation aspects of the quasi-linearized tidal model developed by the Grenoble tidal group. Starting from the hydrodynamic model, which is represented by a linearized wave equation, we emphasize the different steps taken to lead to the final finite-element discrete system of the coupled hydrodynamic and assimilation problem. As the hydrodynamic formulation has been already detailed in many previous publications, we insist especially on the formulation of the assimilation part. The assimilation is based on a general inverse method using an L_2 norm-type cost function, weighted by the use of inverse error covariance operators. The full implications of choosing this kind of cost function are discussed. The least-square problem thus defined is developed by using the representer approach. The representers are a finite set of functions defined on the modeling domain. The solution is sought as a perturbation of the solution to the prior model and it is shown that this perturbation belongs to the vector subspace of finite dimension generated by the representers (i.e., it is a linear combination of the representers). The assimilation problem then involves first solving two systems, called backward and forward systems, to determine the representers. An alternative formulation of the boundary conditions associated with the forward system is developed, as the original one is somewhat unsuited to the finite-element discretization. The three resulting systems are solved under a variational formulation identical to the one of the hydrodynamic problem. Discretization of the assimilation problem, which is entirely described in the general continuous case, is performed as a last step, consistent with that of the hydrodynamic problem. Finally, the coefficients of the linear combination giving the model perturbation are obtained by solving a $K \times K$ system. As an illustration, we propose a realistic application performed on the M_2 tidal elevation problem in the South Atlantic by assimilating tidal gauge data in a solution of the Grenoble model. © 1999 Academic Press

1. INTRODUCTION

A hydrodynamic model for oceanic tides has been under development for about 20 years by the Grenoble tidal group. Many papers have been published regularly concerning the model itself and its applications, as it has evolved from regional seas to global ocean tidal modeling, where both the latest model improvements and results have widely been discussed in the past years (see, for instance, [1–4]). However, recently a major step was taken by implementing assimilation techniques in the global modeling scheme and this resulted in the production of the FES94 [5] and FES95 [6] solutions. At this point, and because of the complexity of the modeling processes, we believe that it is time for a formal description of the entire model. This is the purpose of this paper. It consists in a summary of the hydrodynamic model formulation, a detailed description of which is available from previous publications, plus a precise description of the assimilation model formulation. There is a strong demand for such a detailed description, essentially because oceanographers can now choose from among different tidal models, which can be purely empirical, like some new TOPEX/Poseidon-derived models, or of mixed origins like the OSU model [24], the Boulder model [7, 8], or the Grenoble model (from which FES94 and FES95 solutions are derived). Thus the aim of this paper is to propose a formal overview of the basic equations and their mathematical and numerical treatments in order to provide a clear, consistent view of what the Grenoble model is now.

Despite the fact that the goal of the Grenoble model is to propose an accurate description of oceanic tides based as much as possible on hydrodynamic considerations only, we have found it necessary, in the present state of the art, to use assimilation techniques. Since the first version of the global solutions, we have used a technique acting only on the open boundary conditions [4] which has proved to be efficient in improving the accuracy of the solutions, but not sufficient, essentially because the tidal forcing that we prescribe inside the domain is unchanged by this technique. The possibility of removing the remaining large-scale errors from the model by using altimetric data without affecting the quality of our solutions in the coastal and shelf areas has already been shown (see [9]). Data assimilation can be seen as seeking the best compromise between fitting observations, which we believe to be a fair measurement of the sea truth, and prior knowledge, which we believe to be a fair picture of the tidal mechanics. As will be shown in this paper, we have chosen the general inverse approach combined with a penalty function based on an L_2 norm, leading to a least-square problem. The general inverse approach has been extensively used in physical problems and is very well documented (see, for instance, [10]). The motivation for using the general inverse approach is that basically we assume that we are better able to describe the hydrodynamic model's errors on the forcing term (i.e., the tidal potential) and boundary conditions than on the solution itself (i.e., the error on the tidal elevations derived from the model). The motivations for choosing the L_2 norm to design our penalty function are, first, that it involves solving a linear system and, second, that it can be justified in terms of statistical models (see, for instance, [10, 11]). Moreover, nudging techniques (used by Schwiderski [12] and Kantha [7]), objective analysis, or, more generally, data inversion as used by Jourdin *et al.* [13] and modal basis function methods (as described in [9]) appear to be a particular case of the general inverse approach (as in [14, 15]). The choice of the penalty function and the description of the model and observation error covariance are clearly the critical points of the method. A previous assimilation scheme, also based on the general inverse method, has been specifically developed to be applied to the Grenoble tidal model

and is described in [16]. However, its formulation was found to be limited in practice when applied to oceanic basin-wide domains by the use of necessarily greatly simplified error covariance (i.e., spatially uncorrelated) related to the tidal forcing terms. This is why we have decided to develop the assimilation model presented in the following. In order to reduce the dimension of the data functional minimization problem, we use the representer technique, first introduced for data assimilation in tidal models in [17]. This powerful technique not only rules out the practical need of using only oversimplified covariance, but it allows us to describe the full assimilation procedure in the continuous space and is ideally suited for the variational formulation of the minimization problem.

2. THE CONTINUOUS ASSIMILATION FORMULATION

2.1. The Hydrodynamic Model

The model's hydrodynamic equations are based on the classical spherical shallow water equations. They basically consist of the vertically averaged Navier–Stokes equations, where horizontal viscosity has been neglected. Dissipation is assumed to take place in a thin boundary layer located at the ocean bottom. Nonlinearities arising from advection terms and dissipation are handled by a perturbation approach, which leads to a quasi-linearized harmonic equation system (we are ignoring here some nontrivial developments, which can be found in [18]; however, for short, it is assumed here that we are able in some way to linearize the friction term, with coefficients varying with space: at first order, the advection terms of the astronomic waves are neglected, but appear as the forcing terms in the nonlinear tides equation, which achieves full linearization of the equations). Tidal forcing is given by the gradient of a tidal potential which includes the astronomical potential plus the solid tide, loading, and self-attraction effects. The unknowns of the system are the horizontal velocities and sea level elevation. Because we have eliminated time from the tidal equations (thanks to linearization), we can formulate the real cosine and sine problem into the spectral complex system and thus solve linearly a given tidal wave independently of the others. Consequently, we will not distinguish the tidal wave by any specific index. The 2D momentum equations are derived from the vertically averaged horizontal 3D momentum equations. The classical hydrostatic pressure distribution is assumed. F represents the forcing term according to the wave we intend to solve. For the main oceanic waves, F is the gradient of the total tidal potential (which is in fact a combination of the astronomic potential, the solid earth tide, and their perturbations due to loading and self-attraction effects). In the following, the exact nature of F can be ignored. In the horizontal axis, the linearized momentum equations are given by

$$(j\omega + r)\mu + (r' - f)v + g \frac{1}{a \cos \varphi} \frac{\partial \alpha}{\partial \lambda} = gF_\lambda \quad (1)$$

$$(r'' + f)\mu + (j\omega + r''')v + g \frac{1}{a} \frac{\partial \alpha}{\partial \varphi} = gF_\varphi, \quad (2)$$

where α is the complex tidal elevation where $h(\lambda, \varphi, t) = \text{Re}(\alpha(\lambda, \varphi)e^{i\omega t})$; \mathbf{u} is the complex barotropic tidal velocity, $\mathbf{u} = (\mu, v)$; a is the mean radius of Earth; λ, φ are longitude and latitude; g is the gravity constant; H is the mean depth; ω is the tidal pulsation; f is the Coriolis factor; \mathbf{F} is the complex tidal forcing, $F = (F_\lambda, F_\varphi)$; and r, r', r'', r''' are friction

coefficients, where friction

$$\mathbf{D} = - \begin{bmatrix} r(\lambda, \varphi) & r'(\lambda, \varphi) \\ r''(\lambda, \varphi) & r'''(\lambda, \varphi) \end{bmatrix} \mathbf{u}.$$

The nondiagonal form of the friction coefficient matrix is due to nonlinear interaction between the different tidal waves. In short, the friction of a given constituent is due to its own currents interacting with a bottom boundary layer which itself is generated by one or two dominant waves, i.e., waves whose currents have a much larger amplitude locally than those of the other constituents. In our simulations, $M2$ (the mean lunar semi-diurnal tide, with a period of 12 h, 25 min) and $K1$ (the luni-solar declinational diurnal tide) play the role of the dominant waves generating background turbulence in the ocean bottom boundary layer, on the basis of their leading position (in terms of amplitude) in both species (diurnal and semi-diurnal bands). In other words, the $M2$ tide is responsible for the bottom boundary layer where the semi-diurnal tides are larger than the diurnal tides, and the $K1$ tide plays this role in the opposite conditions. (1) and (2) can be summarized in the form

$$H\mathbf{u} = \mathbf{M}(\nabla\alpha - \mathbf{F}), \quad (3)$$

where

$$\mathbf{M} = -\frac{gH}{\Delta} \begin{bmatrix} i\omega + r''' & f - r' \\ -f - r'' & i\omega + r \end{bmatrix} \quad \Delta = \begin{vmatrix} i\omega + r & r' - f \\ r'' + f & i\omega + r''' \end{vmatrix}.$$

The continuity equation is obtained by expressing the mass conservation of a fluid with uniform density. It is linearized by applying a perturbation technique similar to the one used to linearize the momentum equations. As with the momentum equations, the right-hand term depends on the origin of the computed wave. In short, it is equal to zero in the case of the so-called oceanic tides (like M_2 , S_2 , $K1$, etc.), but not in that of tidal waves of nonlinear origin (like M_4 , MS_4 , etc.). For convenience, and despite the fact that our major interest is the study of oceanic tides, we will keep a general form of the continuity equation

$$i\omega\alpha + \nabla \cdot H\mathbf{u} = F_\alpha. \quad (4)$$

The tidal problem is solved numerically, which obviously implies a particular choice of discretization. In the case of gravity waves, dissipation processes due to bottom friction actually take place mostly in the shallowest areas such as the continental shelves. In these areas, the typical wavelengths are dramatically shorter than in the deep ocean and so spatial resolution of the discretization must be considerably increased in such regions. A uniform high resolution mesh would mean having to solve a huge numerical system, even in regional applications, which is clearly incompatible with the goal of modeling the oceanic barotropic tides on a global scale. This is why we use the finite element discretization, which allows us to constrain the local spatial resolutions by criteria based on dynamic considerations. It has been shown by Lynch that direct resolution of the full set of equations, where elevation and velocity are independent unknown quantities, may lead to an ill-conditioned system [19]. In order to avoid this particular problem, and because our first interest is to determine tidal elevations, the model is confined to the so-called wave equation which is obtained by

eliminating velocity from the continuity equation. Finally, our hydrodynamic model can be written by applying the wave equation at any point \mathbf{x} of our modeling domain Ω ,

$$S[\alpha](\mathbf{x}) = \frac{1}{\kappa}(i\omega\alpha + \nabla \cdot \mathbf{M}\nabla\alpha)(\mathbf{x}) = \psi(\mathbf{x}) = \frac{1}{\kappa}(F_\alpha + \nabla \cdot \mathbf{M}\mathbf{F})(\mathbf{x}), \quad (5)$$

where κ is a normalization factor: $\kappa = \omega a^2(\pi/180)^{-2}$. The boundary conditions along the open limits are the Dirichelet-type conditions $\alpha = \alpha_o$ on $\partial\Omega_o$, and those along the rigid limits are the Neuman-type conditions $H\mathbf{u} \cdot \mathbf{n} = \mathbf{M}(\nabla\alpha - F) \cdot \mathbf{n} = 0$ on $\partial\Omega_c$. As will be discussed below, this system is finally solved in its variational formulation discretized by the using the FE technique (triangular elements, Lagrange-P2 approximation). In the following, the solution of this system will be called the prior solution. Once the elevation is solved, one can derive the associated tidal velocities by applying (3).

2.2. The Assimilation Model

In the following, we will disregard the matter of model precision, and confine ourselves to the problem of model accuracy, which implies that we can obtain the true solution providing we use the true input parameters (i.e., the true right-hand terms in our equations and the true boundary conditions), or, in other words, the necessary simplifications of the model (such as bottom friction parameterization, linearization) have a negligible influence. This is a significant hypothesis, but it is well justified if one has more confidence in the design of the model than in the input parameters, which is exactly the case in this paper. The first step after solving a physical problem is to validate its solutions, in terms of precision and accuracy. One favorite modeling technique to evaluate accuracy is to compare the model's diagnostic outputs with observations. If the validation tests show that the model fits the prior requirements, it is well done. Unfortunately, comparison between the model and the observations mostly shows unsatisfactory misfits, which indicates that the model and/or the data are not accurate enough. But it is indeed a very narrow way of thinking to use observations only for diagnostic validation. After all, they represent valuable information which may be used to improve the model and we would like to assimilate this into the model. As the model is in some ways self-consistent, a general problem involving the model equations plus additional constraints designed to make the model fit the observations exactly would be overdetermined. So data assimilation basically consists in seeking the best compromise between a relaxation of the prior solution and misfits with observations. In fact, data assimilation is a formal approach of the natural, empirical process of comparing model and observations, and deciding from these two sources of information where sea truth stands, given the confidence we have in these two sources. This kind of problem has been largely discussed and studied in the fluid mechanics domain. In this paper, we will present a data assimilation process based on the general inverse technique, using a least-square approach. The least-square approach involves seeking the model perturbation that minimizes a cost function which is based on two L_2 norm-type terms

$$J(\text{model solution perturbation}) = \frac{(\text{misfits with the data})^2}{(\text{data error range})^2} + \frac{(\text{departure from the prior solution})^2}{(\text{model error range})^2}, \quad (6)$$

where the first right-hand term denotes the difference between a new solution, consisting

in a relaxation of the prior model solution, and the observations weighted according to the confidence placed in them, and the second term denotes the departure from the prior model solution weighted according to the confidence placed in it. The latter term is also often called the regularization term. The least-square method is probably the most widely used, essentially because it then involves solving a linear system. Moreover, Tarantola [10] has shown that, under certain conditions (linear, finite dimension model, Gaussian distribution of the model and observation errors), it also can be fully linked with a probabilistic approach. To work out our assimilation, we do not strictly need to justify a particular distribution of the observations and model errors. All that we need is to decide on a set of reasonable weights to use in the cost function. However, it is of great help to relate the cost function design with a probabilistic point of view. Indeed, by using a cost function as in (6), we intrinsically assume that, at any point of the modeling domain and for a given model parameter, the probability distribution for this parameter, if it is to be exact, is a Gaussian one centered on the prior model value. In other words, if we had a mean to determine a large unbiased set of realizations of this parameter, we would statistically obtain a Gaussian distribution centered on the prior model parameter. So the prior model parameters are not assumed to be the truth, but the best unbiased estimator of the truth. A similar interpretation can be made of the observations. The intrinsic assumption of Gaussian distribution is due to the choice of an L_2 norm. Despite the fact that Gaussian distribution is probably one of the physicists' favorites, especially when the actual distribution is not known, it should be handled with caution since it assumes a rapid decrease in probability for the largest errors. Such an assumption can easily break down in real applications. For instance, in the tidal field, we know that many observations show serious errors due to erroneous phase archives. In this paper, however, we will assume that the Gaussian distribution of observation and model errors is mainly satisfactory. Additionally, the meaning and justification of the probabilistic interpretation of the assimilation problem have been extensively discussed by different authors already, so we will simply recall here the main hypotheses and results. The reader can usefully refer to [10] for more details. As pointed out above, we assume that our model errors are due to faulty forcing terms and boundary conditions, the departures of which from prior model values, denoted $(\delta\psi, \delta\alpha_o, \delta\Phi)$, are given by

$$\begin{aligned} \forall \mathbf{x} \in \Omega, & \quad \delta\psi(\mathbf{x}) = \psi(\mathbf{x}) - \psi_{\text{prior}}(\mathbf{x}) \\ \forall \mathbf{x} \in \partial\Omega_o, & \quad \delta\alpha_o(\mathbf{x}) = \alpha_o(\mathbf{x}) - \alpha_{o\text{prior}}(\mathbf{x}) \\ \forall \mathbf{x} \in \partial\Omega_c, & \quad \delta\Phi(\mathbf{x}) = [H(\mathbf{u} - \mathbf{u}_{\text{prior}}) \cdot \mathbf{n}](\mathbf{x}). \end{aligned} \quad (7)$$

The resulting tidal elevation field is given by

$$\forall \mathbf{x} \in \bar{\Omega}, \quad \alpha(\mathbf{x}) = \alpha_{\text{prior}}(\mathbf{x}) + \delta\alpha(\mathbf{x}), \quad (8)$$

where $\delta\alpha$ is the solution of the linear system

$$S[\delta\alpha](\mathbf{x}) = \delta\psi(\mathbf{x}) \quad (9)$$

with the associated boundary conditions $\delta\alpha = \delta\alpha_o$ on $\partial\Omega_o$, and $\mathbf{M}\nabla\delta\alpha \cdot \mathbf{n} = \delta\Phi$ on $\partial\Omega_c$. We assume that $(\delta\psi, \delta\alpha, \delta\Phi)$ is a set of three independent random fields. As mentioned above, they are assumed to be zero-averaged. The assimilation solution is defined by the particular realization of these random variables, which minimizes the cost function. $\delta\psi$ represents the error pending to the right-hand side of the wave equation. It contains the error due to

linearization of the mass conservation law, the error in the divergence of the momentum equation forcing, and other error terms. $\delta\alpha$ represents the error in our previous knowledge of the tidal elevation along the open boundaries. $\delta\Phi$ represents the error resulting from two different sources. The first one is due to an erroneous nonflux condition along the closed boundaries. This can occur when the model limits do not fit the real coastlines well. Due to the FE's ability to follow coastlines very precisely, it should not be considered, except for significantly large river delta limits, where no open boundary condition could reasonably be set (due to the lack of tidal data for example) or for the limits of significantly large bays which are dry during the low tide cycle. The error in the nonflux condition is thus very local and can be mostly disregarded, except in some very special cases. But $\delta\Phi$ also represents the error due to the flux of momentum equation forcing. Using the same forcing terms \mathbf{F} to set wave equation forcing and closed boundary conditions, the problem of a possible correlation between $\delta\Phi$ and $\delta\psi$ will occur, and consequently the validity of considering them as independent random variables. Nevertheless, this affects only the theoretical significance of the definition of the penalty function, and we assume that this problem can be ignored. Only in practical applications must the estimated covariance functions corresponding $\delta\Phi$ and $\delta\psi$ be consistent. Following [24], we assume that the model error statistics can be described approximately by their error covariance functions

$$\begin{aligned} c_i(\mathbf{x}_1, \mathbf{x}_2) &= E[\delta\psi(\mathbf{x}_1)\delta\psi(\mathbf{x}_2)^*] & \forall(\mathbf{x}_1, \mathbf{x}_2) \in \Omega \times \Omega \\ c_o(\mathbf{x}_1, \mathbf{x}_2) &= E[\delta\alpha_o(\mathbf{x}_1)\delta\alpha_o(\mathbf{x}_2)^*] & \forall(\mathbf{x}_1, \mathbf{x}_2) \in \partial\Omega_o \times \partial\Omega_o \\ c_c(\mathbf{x}_1, \mathbf{x}_2) &= E[\delta\Phi(\mathbf{x}_1)\delta\Phi(\mathbf{x}_2)^*] & \forall(\mathbf{x}_1, \mathbf{x}_2) \in \partial\Omega_c \times \partial\Omega_c, \end{aligned} \quad (10)$$

where E is the mathematical expectation, $*$ denotes the conjugate value (transpose conjugate if applied to a vector). Let us suppose that we have a set of K observations. As with the model errors, we suppose that d_k is the best unbiased estimator of the observation (measurement) of α_{true} at \mathbf{x}_k . We then can define the random variable representing the measurement error at the k th observation site, i.e., the departure of an actual measurement m_k from the ‘‘central’’ value d_k :

$$\varepsilon_k = m_k - d_k \quad \text{at } \mathbf{x}_k. \quad (11)$$

As with the model parameter errors, we assume that we can, at least approximately, describe its covariance:

$$c_\varepsilon(\mathbf{x}_k, \mathbf{x}_l) = E[\varepsilon_k \varepsilon_l^*]. \quad (12)$$

In practice, d_k and c_ε can be seen as representing the known statistics of our instrument, or measuring process. As the four random variables are independent, their cross-covariance is equal to zero. In order to simplify the discussion, we will consider only sea elevation harmonic observations in the following. It should be noted that this has no influence on the theoretical development. The data function L_k , associated with the actual observation d_k made at location \mathbf{x}_k , projects the tidal elevation field in the observation space. In our case, because the solution in which we want to assimilate data is a tidal elevation field, it is simply an interpolation of the solution α at location \mathbf{x}_k . Let us define a penalty function J_d for the observations,

$$J_d(\alpha) = \mathbf{e}^* \mathbf{C}_\varepsilon^{-1} \mathbf{e}, \quad (13)$$

where $\mathbf{e} = \mathbf{d} - \mathbf{L}[\alpha] = [d_k - L_k[\alpha]]$, $\mathbf{C}_\varepsilon = [c_\varepsilon(\mathbf{x}_k, \mathbf{x}_l)]$.

The probability density for the measurement of a field α to coincide with the measurement of α_{true} is then given by

$$\rho_d(\alpha) = \frac{1}{\sqrt{(2\pi)^K \det C_\varepsilon}} \exp(-J_d(\alpha)). \quad (14)$$

Let us now define a penalty function J_m for the model. First, for each model error covariance, we define the corresponding linear covariance operator acting on a field α and defined by

$$\begin{aligned} C_i: \psi &\mapsto C_i[\psi] & C_i[\psi](\mathbf{x}) &= \int_{\Omega} c_i(\mathbf{x}, \mathbf{x}') \psi(\mathbf{x}') ds \\ C_o: \alpha &\mapsto C_o[\alpha] & C_o[\alpha](\mathbf{x}) &= \int_{\partial\Omega_o} c_o(\mathbf{x}, \mathbf{x}') \alpha(\mathbf{x}') dl \\ C_c: \Phi &\mapsto C_c[\Phi] & C_c[\Phi](\mathbf{x}) &= \int_{\partial\Omega_c} c_c(\mathbf{x}, \mathbf{x}') \Phi(\mathbf{x}') dl. \end{aligned} \quad (15)$$

Note that the covariance operators are self-adjoint for the canonical scalar products. For instance, this yields for C_i :

$$\langle \psi_1, C_i[\psi_2] \rangle = \int_{\Omega} \psi_1(\mathbf{x}')^* C_i[\psi_2](\mathbf{x}) ds = \int_{\Omega} \{C_i[\psi_1](\mathbf{x}')\}^* \psi_2(\mathbf{x}) ds = \langle C_i[\psi_1], \psi_2 \rangle. \quad (16)$$

Thus J_m take the form

$$\begin{aligned} J_m(\alpha) &= \int_{\Omega} \partial\psi^*(\mathbf{x}) C_i^{-1}[\partial\psi](\mathbf{x}) ds + \int_{\partial\Omega_o} \partial\alpha_o^*(\mathbf{x}) C_o^{-1}[\partial\alpha_o](\mathbf{x}) dl \\ &\quad + \int_{\partial\Omega_c} \delta\Phi^*(\mathbf{x}) C_c^{-1}[\delta\Phi](\mathbf{x}) dl. \end{aligned} \quad (17)$$

We assume here that the covariance operators have all a well-defined inverse. This is a nontrivial assumption, in particular if the error covariance is more or less uniform (in the case of highly correlated errors). The probability density for a set model parameters to be the true model parameters is given by

$$\rho_{md} = A \exp(-J_m(\alpha)), \quad (18)$$

where A is a normalization coefficient. They both represent our two initial independent sources of information, which we want to combine. Taken separately, J_d tells us that the set \mathbf{d} of observation values is the best estimator of the sea truth at the observation sites, and J_m that our prior model is the best estimator of the possible parameters. Combining both sources of information involves determining the field that produces the maximum likelihood for the probability density given by

$$\rho_{md} = B \exp[-(J_d(\alpha) + J_m(\alpha))], \quad (19)$$

where B is a normalization factor. In other words, the assimilation solution is obtained by minimizing a penalty function defined by

$$J(\alpha) = J_d(\alpha) + J_m(\alpha). \quad (20)$$

The solution can be obtained by many different techniques. In practice, discretizing the assimilation problem by straightforward techniques requires us to express the inverse covariance functions explicitly. In most cases, a modeler has only an (approximate!) knowledge of the covariance functions themselves, based on statistical considerations for instance. So we will usually establish the covariances, and then inverse them. If the number of computational nodes is large, and if correlation lengths are not short compared to the spatial resolution, this will result in the inversion of huge, nontrivial matrices. This has been the reason for former data assimilation to be performed by poor, physically unacceptable covariance functions, artificially simplified by shortening the correlation length. We found this approach to be unsatisfactory, as the quality of the assimilation depends essentially on the quality of the error descriptions via the covariance functions. For instance, if the model is contaminated by a large wavelength error (i.e., the spatial scale is of the order of the domain size or greater), one can expect to improve it by using only a few observations, and the model's error covariance functions will take care of "propagating" the sparse information throughout the domain. However, by using simplified, decorrelated covariance, this cannot be done, and it becomes more likely that the solution will be modified only in the vicinity of the observations, creating artificial peaks around observation locations and leaving the rest of the prior solution unchanged. So not only does the solution not improve very much, it is also degraded by the introduction of nonphysical features. It must be clearly understood that the role of the covariance functions is essential, particularly in nonideal (say practical) applications, where observations are very likely to be poorly distributed over the modeling domain.

2.2.1. The representer technique. The principle of the representer technique, adapted to the tidal problem, has already been extensively presented in the literature (see, for instance, [20–24]) and so only the basic aspects of this technique will be recalled here. Let us define the Sobolev space $H_1(\Omega)$ of the complex-valued functions, the first derivatives of which are square integrable in the modeling domain Ω . $H_1(\Omega)$ represents the space of the possible tidal elevation. As will be stated in Section 3, the existence and uniqueness of the wave equation solution (in its variational formulation) are guaranteed by certain assumptions of smoothness and orders of magnitude for the friction coefficients, depths, and forcing terms. With additional assumptions it can easily be seen that the existence and uniqueness in $H_1(\Omega)$ of the assimilation problem solution are similarly guaranteed (see end of Section 2.2.3). The penalty function defined by (20) is a positive-definite quadratic form from which we can define an inner product for the space $H_1(\Omega)$:

$$\begin{aligned} \langle \alpha_1, \alpha_2 \rangle_C &= \int_{\Omega} (S[\alpha_1])^* C_i^{-1} [S[\alpha_2]] ds + \int_{\partial\Omega_o} \alpha_1^* C_o^{-1} [\alpha_2] dl \\ &+ \int_{\partial\Omega_c} (\mathbf{M}\nabla\alpha_1 \cdot \mathbf{n})^* C_c^{-1} [\mathbf{M}\nabla\alpha_2 \cdot \mathbf{n}] dl. \end{aligned} \quad (21)$$

The cost function can then be expressed as

$$J(\alpha) = (\mathbf{d} - \mathbf{L}[\alpha])^* \mathbf{C}_\varepsilon^{-1} (\mathbf{d} - \mathbf{L}[\alpha]) + \|\alpha - \alpha_{\text{prior}}\|_C^2. \quad (22)$$

With certain assumptions regarding the regularity of the covariance operators, the inner product given in Eq. (21) is an inner product for $H_1(\Omega)$. $H_1(\Omega)$ is then a Hilbert space (a more detailed justification can be found in [24]). Thus, because the L_k functional is linear,

there exists a field r_k in $H_1(\Omega)$ such that

$$\forall \alpha, \quad L_k[\alpha] = \langle r_k, \alpha \rangle_C, \quad (23)$$

where r_k is the so-called data representer associated with the data functional L_k . Provided that the representers are linearly independent (which we will assume), they form a basis of a vector space V . Any field of $H_1(\Omega)$ can then be expressed as

$$\forall \alpha, \quad \alpha = \alpha_V + \alpha_{V^\perp}, \quad (24)$$

where V^\perp is the vector space orthogonal to V . The following two properties of this breakdown are then noted:

$$\|\alpha\|_C^2 = \|\alpha_V\|_C^2 + \|\alpha_{V^\perp}\|_C^2 \quad (25)$$

$$L_k[\alpha] = \langle r_k, \alpha \rangle_C = \langle r_k, \alpha_V \rangle_C + 0 = L_k[\alpha_V]. \quad (26)$$

Hence the orthogonal term in (24) does not affect the first term of the cost function, and it can be arbitrarily chosen as being equal to the zero field, so it minimizes the right-hand term in (22). The solution is then sought as a linear combination of the data representers, i.e.,

$$\alpha(\mathbf{x}) = \alpha_{\text{prior}}(\mathbf{x}) + \sum_{k=1}^K b_k r_k(\mathbf{x}). \quad (27)$$

At this point, we have reduced the minimization problem from an infinite dimension to a finite dimension, with K degrees of freedom. The cost function simplifies to

$$J(\alpha) = (\mathbf{d} - \mathbf{L}[\alpha])^* \mathbf{C}_\varepsilon^{-1} (\mathbf{d} - \mathbf{L}[\alpha]) + \mathbf{b}^* \mathbf{R} \mathbf{b}, \quad (28)$$

where $R_{ij} = \langle r_i, r_j \rangle_C = L_i[r_j] = \langle r_j, r_i \rangle_C^* = L_j^*[r_i]$. \mathbf{R} is the hermitian representer matrix. The b_k coefficients which minimize (28) are thus solutions of the $K \times K$ system:

$$(\mathbf{R} + \mathbf{C}_\varepsilon) \mathbf{b} = \mathbf{e}_{\text{prior}}. \quad (29)$$

The representers are obtained by solving (23), and the b coefficients are then computed from (29). The error covariance matrix associated with the assimilation solution is then

$$\mathbf{C} = (\mathbf{R}^{-1} + \mathbf{C}_\varepsilon^{-1})^{-1}. \quad (30)$$

As will be shown later, the posterior covariance matrix is a very interesting product of the assimilation. Among other things, it enables us to diagnose the consistency of the prior covariance given for the observations and the model.

2.2.2. A simplified example. At this stage the theoretical problem is completely defined. Nevertheless, the formulation may obscure the basic simplicity of the assimilation model. In the following, we will restrict ourselves to the particular case where the only type of assimilated data are tidal constants. This is not a severe restriction, as most of the accurate tide-related observations we know of are tidal elevation observations and/or model-gridded

solutions, and this has the great advantage of allowing an explicit expression for the corresponding representers (in fact, this is the case when data are point-wise estimates of the hydrodynamic model variable, i.e., the tidal elevation α in our case). First, we temporarily consider a simplified model (i.e., without boundary conditions)

$$\forall \mathbf{x} \in \Omega, \quad S[\alpha](\mathbf{x}) = \psi(\mathbf{x}). \quad (31)$$

It will be recalled that the hydrodynamic operator S is assumed to be exact and all elevation errors are due to errors in the forcing, i.e.,

$$S[\delta\alpha] \equiv \delta\psi. \quad (32)$$

The elevation error covariance function throughout the domain, including the domain boundaries, is defined as

$$\forall(\mathbf{x}, \mathbf{x}') \in \Omega \times \Omega, \quad c_{\alpha,\alpha}(\mathbf{x}, \mathbf{x}') = E(\delta\alpha(\mathbf{x})\delta\alpha^*(\mathbf{x}')). \quad (33)$$

As indicated previously, a linear operator C_i is associated with the error covariance $c_i(\mathbf{x}, \mathbf{x}')$. The penalty function is given by

$$J(\alpha) = \mathbf{e}^* \mathbf{C}_\varepsilon^{-1} \mathbf{e} + \int_{\Omega} \delta\psi^*(\mathbf{x}) C_i^{-1} [\delta\psi](\mathbf{x}) ds. \quad (34)$$

Similarly, we can define an operator C_α ,

$$C_\alpha: \theta \mapsto C_\alpha[\theta] \quad C_\alpha[\theta](\mathbf{x}) = \int_{\Omega} c_{\alpha,\alpha}(\mathbf{x}, \mathbf{x}') \theta(\mathbf{x}') ds, \quad (35)$$

where $c_{\alpha,\alpha}$ is the error covariance function associated with the tidal elevation. Let us define S^\diamond the adjoint operator of S (adjoint for the canonical scalar product) by

$$\forall(\alpha, \beta), \quad \langle S[\alpha], \beta \rangle = \langle \alpha, S^\diamond[\beta] \rangle. \quad (36)$$

Then, as can be easily demonstrated, the C_i and C_α operators are related by

$$\forall\psi, \quad C_i[\psi] = (S \circ C_\alpha \circ S^\diamond)[\psi] \quad (37)$$

Thus the penalty function can be expressed equivalently by

$$J(\alpha) = \mathbf{e}^* \mathbf{C}_\varepsilon^{-1} \mathbf{e} + \int_{\Omega} \delta\psi^* C_i^{-1} [\delta\psi] ds = \mathbf{e}^* \mathbf{C}_\varepsilon^{-1} \mathbf{e} + \int_{\Omega} \delta\alpha^* C_\alpha^{-1} [\delta\alpha] ds. \quad (38)$$

L_k , the observation operator associated with a tidal observation at \mathbf{x}_k , can be written in the general form

$$L_k: \alpha \mapsto L_k(\alpha) = \int_{\Omega} \mu_k^*(\mathbf{x}) \alpha(\mathbf{x}) ds, \quad (39)$$

where μ is allowed to be a Dirac function. In the context of the restriction mentioned above (observations consist only of tidal elevation data), we can write

$$L_k(\alpha) = \alpha(\mathbf{x}_k); \quad (40)$$

thus μ takes exactly the form

$$\mu_k(\mathbf{x}) = \delta_{\mathbf{x}_k}(\mathbf{x}) = \delta(\mathbf{x} - \mathbf{x}_k). \quad (41)$$

By definition,

$$\forall \alpha, \quad L_k(\alpha) = \langle r_k, \alpha \rangle_C = \langle r_k, C_\alpha^{-1}[\alpha] \rangle = \langle C_\alpha^{-1}[r_k], \alpha \rangle. \quad (42)$$

Thus it yields the fundamental and general result

$$\forall \mathbf{x} \in \Omega, \quad r_k(\mathbf{x}) = C_\alpha[\mu_k](\mathbf{x}) = \int_{\Omega} c_\alpha(\mathbf{x}, \mathbf{x}') \mu_k(\mathbf{x}') ds = L^*(c_\alpha(\cdot, \mathbf{x})). \quad (43)$$

In the point-wise case, this is equivalent to

$$\forall \mathbf{x} \in \Omega, \quad r_k(\mathbf{x}) = c_{\alpha, \alpha}(\mathbf{x}, \mathbf{x}_k). \quad (44)$$

So the representer of the data k is actually the error covariance function between the model elevation error at any position \mathbf{x} in the domain and the model elevation error at the data k location \mathbf{x}_k . This clearly demonstrates the fact that objective analysis (where error covariance would be given directly for the tidal elevation) is a particular case of the general inverse approach. The \mathbf{R} matrix is then trivial:

$$\mathbf{R} = [R_{ij}] = [c_{\alpha, \alpha}(\mathbf{x}_i, \mathbf{x}_j)]. \quad (45)$$

Finally, the b coefficients depend only on the model and observation error covariance at the observation locations. More strikingly, $\mathbf{C} = \mathbf{R} + \mathbf{C}_\varepsilon$ represents the total error (model errors at observation sites plus observational errors) covariance matrix. The new “sea truth” at observation location xk is then given by

$$\alpha(\mathbf{x}_k) = \alpha_{\text{prior}}(\mathbf{x}_k) + \sum_{l=1}^K b_l c_{\alpha, \alpha}(\mathbf{x}_k, \mathbf{x}_l) = \alpha_{\text{prior}}(\mathbf{x}_k) + {}^t [c_{\alpha, \alpha}(\mathbf{x}_k, \mathbf{x}_l)] (\mathbf{C}^{-1} \mathbf{e}_{\text{prior}}), \quad (46)$$

where

$${}^t [c_{\alpha, \alpha}(\mathbf{x}_k, \mathbf{x}_l)] = [c_{\alpha, \alpha}(\mathbf{x}_k, \mathbf{x}_l) \cdots c_{\alpha, \alpha}(\mathbf{x}_k, \mathbf{x}_l) \cdots c_{\alpha, \alpha}(\mathbf{x}_k, \mathbf{x}_K)].$$

In vector form, this can be expressed as

$$[\alpha(\mathbf{x}_k)] = [\alpha(\mathbf{x}_k)]_{\text{prior}} + \mathbf{R} \mathbf{b} = \mathbf{C}^{-1} \mathbf{C}_\alpha [\alpha(\mathbf{x}_k)]_{\text{prior}} + \mathbf{C}^{-1} \mathbf{C}_\varepsilon \mathbf{d}, \quad (47)$$

where $[\alpha(\mathbf{x}_k)] = {}^t [\alpha(\mathbf{x}_1) \cdots \alpha(\mathbf{x}_k) \cdots \alpha(\mathbf{x}_K)]$. A similar expression can be written from the observation point of view:

$$[\alpha(\mathbf{x}_k)] = \mathbf{d} - \mathbf{C}_\varepsilon \mathbf{b}. \quad (48)$$

From (47), the barycentric-like nature of the new “sea truth” determination is obvious. In conclusion, the assimilation first computes a “best” compromise at observation locations between observations and the prior model, using arbitrary, prior error covariance. In this

process, both sources of information, i.e., the observations and the prior model, play a very similar role. As a second step, the new model is derived from the observation location by using (27). It appears clearly that, away from any observation point, the added terms depend on the arbitrary choice of the domain-wise covariance functions, with restricted control from the first assimilation step. This choice is therefore crucial to the success of the assimilation in terms of general improvement over the modeling domain. In the particular case of objective analysis, the covariance functions are usually taken to be hat-shaped, the typical radii of which are based on physical considerations. In the general inverse case, we simply take an additional step which consists in computing the elevation error covariance functions from the forcing error covariance functions by using the model equations.

2.2.3. The general inverse problem. Solving the assimilation problem calls for prior determination of the data representers. Each representer is determined separately, so we will omit the data index in the following. L can be written in the general form

$$L(\alpha) = \int_{\Omega} \mu^*(\mathbf{x})\alpha(\mathbf{x}) ds + \int_{\partial\Omega} \nu^*(\mathbf{x})\alpha(\mathbf{x}) dl, \quad (49)$$

where μ and ν are allowed to Dirac functions. For convenience, an intermediate function η is introduced. This is defined by

$$\eta = C_i^{-1}[S[r]]. \quad (50)$$

The representer r is then defined by the equation

$$\forall \alpha, \quad \langle r, \alpha \rangle_C = \int_{\Omega} \eta^* S[\alpha] dS + \int_{\partial\Omega_0} r^* C_o^{-1}[\alpha] dl + \int_{\partial\Omega_c} (\mathbf{M}\nabla r \cdot \mathbf{n})^* C_c^{-1}[\mathbf{M}\nabla\alpha \cdot \mathbf{n}] dl. \quad (51)$$

\mathbf{M}^* the adjoint matrix of the matrix operator \mathbf{M} is defined by $\langle \mathbf{u}, \mathbf{M}\mathbf{v} \rangle = \langle \mathbf{M}^*\mathbf{u}, \mathbf{v} \rangle$. \mathbf{M}^* is the transpose conjugate matrix of \mathbf{M} . In our case, it can easily be seen that

$$\mathbf{M}^* = -\frac{gH}{\Delta^*} \begin{bmatrix} -i\omega + r''''^* & f - r''^* \\ -f - r''^* & -i\omega + r^* \end{bmatrix}. \quad (52)$$

The first part of the scalar product is then transformed. Integrating by parts leads to

$$\int_{\Omega} \eta^* S[\alpha] dS = \int_{\Omega} (S^{\diamond}[\eta])^* \alpha ds + \frac{1}{\kappa} \oint_{\partial\Omega} \eta^* \mathbf{M}\nabla\alpha \cdot \mathbf{n} dl - \frac{1}{\kappa} \oint_{\partial\Omega} \alpha (\mathbf{M}^* \nabla\eta)^* \cdot \mathbf{n} dl, \quad (53)$$

where S^{\diamond} defines the adjoint operator of S :

$$S^{\diamond}[\eta] = \frac{1}{\kappa} (-i\omega\eta + \nabla \cdot \mathbf{M}^* \nabla\eta). \quad (54)$$

Using the self-adjoint properties of the covariance operators, we can transform the remaining terms of (51) into

$$\begin{aligned} & \int_{\partial\Omega_0} r^* C_o^{-1}[\alpha] dl + \int_{\partial\Omega_c} (\mathbf{M}\nabla r \cdot \mathbf{n})^* C_c^{-1}[\mathbf{M}\nabla\alpha \cdot \mathbf{n}] dl \\ & = \int_{\partial\Omega_0} (C_o^{-1}[r])^* \alpha dl + \int_{\partial\Omega_c} (C_c^{-1}[\mathbf{M}\nabla r \cdot \mathbf{n}])^* \mathbf{M}\nabla\alpha \cdot \mathbf{n} dl. \end{aligned} \quad (55)$$

In order to simplify the following developments, we set $\mathbf{M}\nabla\alpha = \vec{\alpha}$, $\mathbf{M}\nabla r = \vec{r}$, $\mathbf{M}^*\nabla\eta = \vec{\eta}$. Finally the representer r is the solution of the equation

$$\begin{aligned} \forall\alpha, \quad \int_{\Omega} \mu^* \alpha \, ds + \oint_{\partial\Omega} v^* \alpha \, dl &= \int_{\Omega} (S^{\diamond}[\eta])^* \alpha \, ds + \frac{1}{\kappa} \oint_{\partial\Omega} (\eta^* \vec{\alpha} - \alpha \vec{\eta}^*) \cdot \mathbf{n} \, dl \\ &+ \int_{\partial\Omega_o} (C_o^{-1}[r])^* \alpha \, dl \\ &+ \int_{\partial\Omega_c} (C_c^{-1}[\vec{r} \cdot \mathbf{n}])^* \vec{\alpha} \cdot \mathbf{n} \, dl. \end{aligned} \quad (56)$$

We seek a suitable solution for η and r . As the above equation must apply for any α , it can easily be seen that we can separate the surface integral terms from the along-boundary integral terms. Identifying term by term leads to the following two equations:

$$\forall\alpha, \quad \int_{\Omega} \mu^* \alpha \, ds = \int_{\Omega} (S^{\diamond}[\eta])^* \alpha \, ds \quad (57)$$

$$\begin{aligned} \forall\alpha, \quad \oint_{\partial\Omega} v^* \alpha \, dl &= \frac{1}{\kappa} \oint_{\partial\Omega} (\eta^* \vec{\alpha} - \alpha \vec{\eta}^*) \cdot \mathbf{n} + \int_{\partial\Omega_o} (C_o^{-1}[r])^* \alpha \, dl \\ &+ \int_{\partial\Omega_c} (C_c^{-1}[\vec{r} \cdot \mathbf{n}])^* \vec{\alpha} \cdot \mathbf{n} \, dl. \end{aligned} \quad (58)$$

From (58) we obtain

$$S^{\diamond}[\eta] = \mu. \quad (59)$$

This equation is a differential equation and η appears to be the response of the adjoint wave equation to an impulse μ . In the context of this paper, μ is the Dirac function associated with the spatial location \mathbf{x}_d . The second equation is similar to a boundary condition. The boundary condition equation is then considered in two parts (rigid and open boundary). The theoretical problem is now completely defined, and the representer is determined by solving two successive sets of differential equations with their associated boundary conditions. First the impulse response η is determined by solving the system (59) with the corresponding boundary conditions $\eta = 0$ on $\partial\Omega_o$ and $\vec{\eta} \cdot \mathbf{n} = -\kappa v$ on $\partial\Omega_c$. It may be noticed that η does not depend on the description of model and data error covariances. Once the η system has been solved, the representer can then be determined by solving the system

$$S[r] = C_i[\eta] \quad (60)$$

with the corresponding boundary conditions $r = C_o[v + 1/\kappa \vec{\eta} \cdot \mathbf{n}]$ on $\partial\Omega_o$ and $\vec{r} \cdot \mathbf{n} = 1/\kappa C_c[\eta]$ on $\partial\Omega_c$. (27) can be formulated in a different manner as

$$\psi(\mathbf{x}) = \psi_{\text{prior}}(\mathbf{x}) + \sum_{k=1}^K b_k C_i[\eta_k](\mathbf{x}), \quad (61)$$

which shows that the assimilation solution is that of the wave equation forced by the prior forcing plus a linear combination of the smoothed η functions (and also modified boundary conditions). As a consequence, the conditions of existence and uniqueness of the assimilation solution are similar to those of the solution to the direct hydrodynamic problem.

2.2.4. *Modifying the representers open boundary conditions.* Unfortunately, the boundary condition involved the gradient of η , which is not very well suited to the FE formulation (due to the pathological noncontinuity of the normal gradient along the element sides, in most of the classical polynomial approximations, Lagrange-P2 in our case). In addition to this fact, more gradient discontinuity may occur if the limits are not straight, due to the fact that the normal and tangential directions are then ill-defined at the limit corners. From experience, direct application of this formulation leads to an inaccurate solution of the representer, with significant consequences on the assimilation solution, in the case of straight limits or not. We therefore wish to transform it for practical reasons. As is shown in the Appendix, it can be expressed as

$$\forall \mathbf{x} \in \partial\Omega_o, r(\mathbf{x}) = \int_{\Omega} c_{\alpha,\alpha}(\mathbf{x}, \mathbf{x}') \mu(\mathbf{x}') ds + \int_{\partial\Omega} c_{\alpha,\alpha}(\mathbf{x}, \mathbf{x}') v(\mathbf{x}') dl = L(c_{\alpha,\alpha}(\mathbf{x}, \cdot)). \quad (62)$$

If we assimilate tidal elevation data (i.e., the image of a function by the observation operator L is its value at location \mathbf{x}_{data}), the open boundary condition applied to the representer associated with the observation located at \mathbf{x}_{data} reduces to

$$\forall \mathbf{x} \in \partial\Omega_o, \quad r(\mathbf{x}) = c_{\alpha,\alpha}(\mathbf{x}, \mathbf{x}_{\text{data}}); \quad (63)$$

$c_{\alpha,\alpha}(\mathbf{x}, \mathbf{x}_{\text{data}})$ itself can be obtained by solving the system (A4), which is similar to a hydrodynamic system forced only by the open boundaries. This result clearly shows that the value of the representers along the open limits depends only on the covariance function related to the open boundary condition errors propagated inside the domain by the hydrodynamic model. It also explicitly establishes the link between the representer approach and the technique for open boundary condition optimization described in [4].

3. THE VARIATIONAL FORMULATION

As mentioned previously, the wave equation is solved by its variational formulation. Considering the Sobolev space $H^1(\Omega)$ of the complex-valued functions, the first derivatives of which are square-integrable in the domain Ω , we introduce a subspace of $H^1(\Omega)$ defined by

$$W_{\partial\Omega_o}(\beta_o) = \{\beta \in H^1(\Omega) : \beta = \beta_o \text{ on } \partial\Omega_o\}. \quad (64)$$

The variational formulation is obtained by integrating the differential equation multiplied by a test function β of $W_{\partial\Omega_o}(0)$ throughout the domain

$$\forall \beta \in W_{\partial\Omega_o}(0), \quad \int_{\Omega} \beta^* S[\alpha] ds = \int_{\Omega} \beta^* \psi ds. \quad (65)$$

Integrating by parts and considering the boundary conditions on α , β , and \mathbf{u} leads to the final variational problem, where the nonflux condition on the rigid boundary is now natural,

$$\begin{aligned} \forall \beta \in W_{\partial\Omega_o}(0), \quad & \frac{1}{\kappa} \int_{\Omega} i\omega \beta^* \alpha ds - \frac{1}{\kappa} \int_{\Omega} \nabla \beta^* \cdot \mathbf{M} \nabla \alpha ds \\ & = \frac{1}{\kappa} \int_{\Omega} (\beta^* F_{\alpha} - \nabla \beta^* \cdot \mathbf{M} \mathbf{F}) ds, \end{aligned} \quad (66)$$

with the boundary conditions $\alpha = \alpha_o$ on $\partial\Omega_o$ (note that the rigid boundary conditions are now implicitly included in the tidal elevation problem). In a similar manner to the hydrodynamic formulation, we can derive the final formulation for the variational backward and forward problem,

$$\begin{aligned} \forall \beta \in W_{\partial\Omega_o}(0), \quad & \frac{1}{\kappa} \int_{\Omega} -i\omega\beta^* \eta \, ds - \frac{1}{\kappa} \int_{\Omega} \nabla\beta^* \cdot \mathbf{M}^* \nabla\eta \, dS \\ & = \int_{\Omega} \beta^* \mu \, dS + \oint_{\partial\Omega_c} \beta^* \nu \, dl, \end{aligned} \quad (67)$$

with the boundary conditions $\eta = 0$ on $\partial\Omega_o$ and

$$\begin{aligned} \forall \beta \in W_{\partial\Omega_o}(0), \quad & \frac{1}{\kappa} \int_{\Omega} i\omega\beta^* r \, ds - \frac{1}{\kappa} \int_{\Omega} \nabla\beta^* \cdot \vec{\mathbf{r}} \, ds \\ & = \int_{\Omega} \beta^* C_i[\eta] \, ds + \frac{1}{\kappa^2} \int_{\partial\Omega_c} \beta^* C_c[\eta] \, dl, \end{aligned} \quad (68)$$

with the boundary conditions $r = C_o[v + \frac{1}{\kappa}\vec{\eta} \cdot \mathbf{n}]$ on $\partial\Omega_o$. As pointed out previously, we wish to avoid having to compute the gradient of η by using the alternative boundary condition formulation (63). Therefore we need to compute the covariance function $c_{\alpha,\alpha}(\mathbf{x}_o, \mathbf{x}_{\text{data}})$ for any given \mathbf{x}_o belonging to the open boundary. To do so, we build a model for $c_{\alpha,\alpha}(\mathbf{x}_o, \mathbf{x})$ considered as a function of \mathbf{x} . Let us define the function c :

$$\forall \mathbf{x} \in \Omega, \quad c(\mathbf{x}) = c_{\alpha,\alpha}^*(\mathbf{x}_o, \mathbf{x}). \quad (69)$$

As shown in the Appendix, this is the solution of the system

$$S[c] = \frac{1}{\kappa} (i\omega c + \nabla \cdot \vec{\mathbf{c}}) = 0, \quad (70)$$

with the boundary conditions $c(\mathbf{x}) = c_o^*(\mathbf{x}_o, \mathbf{x}) \, \forall \mathbf{x} \in \partial\Omega_o$ and $\vec{\mathbf{c}} \cdot \mathbf{n} = 0$ on $\partial\Omega_c$, where $\vec{\mathbf{c}} = \mathbf{M}\nabla c$. Its variational formulation is then

$$\forall \beta \in W_{\partial\Omega_o}(0), \quad \frac{1}{\kappa} \int_{\Omega} i\omega\beta^* c \, ds - \frac{1}{\kappa} \int_{\Omega} \nabla\beta^* \cdot \vec{\mathbf{c}} \, ds = 0, \quad (71)$$

with the boundary conditions $c(\mathbf{x}) = c_o^*(\mathbf{x}_o, \mathbf{x}) \, \forall \mathbf{x} \in \partial\Omega_o$. In theory, this system has to be solved for each boundary node, and the solution field must be interpolated at each data location. However, the computational cost can be lowered by computing the impulse response (or Green function) of the direct hydrodynamic system once and for all for each boundary node.

4. THE DISCRETE PROBLEM

The hydrodynamic and assimilation problems are now fully described. Discretization and solution by computer may be seen as secondary aspects. But this is in fact not the case, and we intend to point out here some delicate matters involved in discretization. In the following, we assume that all quantities to be computed are sought in their discrete form,

$$\alpha(x) = \sum_N \alpha_n \beta_n(x) \quad r(x) = \sum_N r_n \beta_n(x) \quad \eta(x) = \sum_N \eta_n \beta_n(x),$$

where $\{\beta_n\}$ is the set of interpolation functions (for instance P2-Lagrange real-valued polynomials) related to the nodes of the finite element mesh. In order to simplify the notation, we will denote

$$\beta(x) = \begin{bmatrix} \beta_1(x) \\ \vdots \\ \beta_N(x) \end{bmatrix} \quad \tilde{\alpha} = \begin{bmatrix} \alpha_1 \\ \vdots \\ \alpha_N \end{bmatrix} \quad \tilde{r} = \begin{bmatrix} r_1 \\ \vdots \\ r_N \end{bmatrix} \quad \tilde{\eta} = \begin{bmatrix} \eta_1 \\ \vdots \\ \eta_N \end{bmatrix}.$$

4.1. Covariance Operator and Scalar Product Discretization

Discretization of the covariance operators may appear to be a minor problem. This is not the case, since we know from experience that rough discretization can have catastrophic effects on assimilation. The main reason is the intrinsic relationship $L_i[r_j] = L_j^*[r_i]$, which is exact in theory, but not if the forcing and boundary conditions of the forward problem, derived by applying the error covariance operators, are not handled with care. As a result of unsuitable discretization, the \mathbf{R} matrix is no longer hermitian and the solution of (29) can be seriously affected. So the aim of this section is to propose a consistent discretization of the covariance operators. By definition,

$$C[\alpha](x) = \int_{\Omega} c(x, x') \alpha(x') ds = \sum_N \alpha_n \int_{\Omega} c(x, x') \beta_n(x') ds. \quad (72)$$

The scalar product related to the covariance operator C of two discretized elevation fields is discretized exactly by

$$\langle \alpha_1, \alpha_2 \rangle_C = \int_{\Omega} \alpha_1^*(x) C[\alpha_2](x) ds = \tilde{\alpha}_1^* [(\beta_m, \beta_n)_C] \tilde{\alpha}_2. \quad (73)$$

Discretization of the covariance operator itself is not an easy matter. Even if it is applied to a Pn-Lagrange function, the image function is not guaranteed to be a Pn-Lagrange function as well. For practical reasons, we would prefer to use a covariance operator which actually preserves the discretization. A full description can be found in the Appendix, and just the main points are given here. Let us define the ‘‘covariance matrix’’ \mathbf{C} associated with the covariance c by

$$\mathbf{C} = [c_{m,n}] = [c(\mathbf{x}_m, \mathbf{x}_n)]. \quad (74)$$

The proper discretized covariance function can then be expressed as

$$\tilde{c}(\mathbf{x}, \mathbf{x}') = \beta^*(\mathbf{x}) \mathbf{C} \beta(\mathbf{x}'). \quad (75)$$

Let us define the real symmetric (hence hermitian) \mathbf{B} matrix:

$$B_{n,l} = \int_{\Omega} \beta_n(\mathbf{x}) \beta_l(\mathbf{x}) ds. \quad (76)$$

The covariance operator can then be loosely expressed in a discrete way by

$$C: \tilde{\alpha} \mapsto C[\tilde{\alpha}] = \mathbf{C} \mathbf{B} \tilde{\alpha}. \quad (77)$$

From the discrete formulation of the covariance operator, we can obtain the concise discrete expression of the C -scalar product:

$$\langle \alpha_1, \alpha_2 \rangle_C = \tilde{\alpha}_1^* \mathbf{BCB} \tilde{\alpha}_2. \quad (78)$$

Because the \mathbf{B} and \mathbf{C} matrices are hermitian, \mathbf{BCB} is also hermitian. We have described here the discretization of the covariance operator for the interior (forcing) error which is consistent with model discretization, denoted $\mathbf{BC}_f \mathbf{B}$ in the following. A similar kind of discretization can obviously be applied to the covariance operators related to the rigid, denoted $\mathbf{BC}_c \mathbf{B}$ in the following, and open boundary condition errors, denoted \mathbf{C}_o in the following. In practice, the smoothing step turns out to be one of the hard parts of the assimilation process because of the size of the \mathbf{CB} matrix, and it calls for special attention. If the error covariance is assumed to have a normal spatial distribution, the smoothing process can be performed by using a technique based on a diffusion equation (see [24]). Instead of multiplying the η fields once with a huge, nearly full matrix, this technique involves multiplying the η fields with a narrow band matrix several times (depending on the required degree of smoothness of error covariance).

4.2. Model Discretization

The subset of $\{\beta_n\}$ related to nodes not located on the open boundary is a basis of the vector space of the second-degree polynomial functions defined over the domain, which have a value of zero along the open boundary. The hydrodynamic and assimilation linear systems are discretized by prescribing any element of this basis to verify the differential systems separately. The linear system of discrete equations is completed by prescribing the boundary conditions. In practice, it is more convenient as a first step to assemble the whole system without distinguishing boundary and interior nodes and obtain what we call the differential matrix of the forward system,

$$\mathbf{S} = [s_{m,n}] = \left[\frac{1}{\kappa} \int_{\Omega} (i\omega \beta_m^* \beta_n - \nabla \beta_m^* \cdot \mathbf{M} \beta_n) a^2 \cos \varphi \, d\lambda \, d\varphi \right], \quad (79)$$

and the same is true for the right-hand side term:

$$\mathbf{Y} = [y_m] = \left[\frac{1}{\kappa} \int_{\Omega} \left(\beta_m^* \sum_N F_n^\alpha \beta_n - \nabla \beta_m^* \cdot \mathbf{M} \left(\sum_N \mathbf{F}_n \beta_n \right) \right) a^2 \cos \varphi \, d\lambda \, d\varphi \right]. \quad (80)$$

We also have to apply the open boundary conditions. To simplify notation, we assume that the open boundary nodes are indexed from 1 to N_o and the interior and rigid boundary nodes are indexed $N_o + 1$ to N in the mesh node numbering. The matrix S and the right-hand side term can be split into blocks as follows:

$$\mathbf{S} = \begin{bmatrix} 1 & 0 \\ \mathbf{S}_{2,1} & \mathbf{S}_{2,2} \end{bmatrix} \quad \text{and} \quad \mathbf{Y} = \begin{bmatrix} \alpha_o \\ f \end{bmatrix}.$$

For the hydrodynamic system, we get

$$\mathbf{S} \tilde{\alpha} = \mathbf{Y}. \quad (81)$$

The integrals are computed piece-wise on the mesh elements, by numerical methods which consist of a weighted sum of the value of the function to be integrated at special points inside the elements (Hammer formula). Therefore, the gradient involved in the terms below the integral signs is computed strictly inside the elements and we thus avoid the gradient non-continuity obstacle. Solving the assimilation problem (backward + forward) does not involve recomputing any differential matrix. Indeed, if we disregard the specific treatment due to the boundary conditions, then it can easily be seen that the matrix of the adjoint of the discrete problem is the adjoint matrix (transpose conjugate) of the discrete problem:

$$\begin{aligned} (s^\diamond)_{m,n} &= \frac{1}{\kappa} \int_{\Omega} \{-i\omega\beta_n\beta_m^* + \nabla\beta_m^* \cdot \mathbf{M}^* \nabla\beta_n\} a^2 \cos\varphi \, d\lambda \, d\varphi \\ &= \frac{1}{\kappa} \int_{\Omega} \{(i\omega\beta_n^*\beta_m)^* + (\mathbf{M}\nabla\beta_m \cdot \nabla\beta_n^*)^*\} a^2 \cos\varphi \, d\lambda \, d\varphi = (s_{n,m})^*. \end{aligned} \quad (82)$$

So it is of great interest to save the overall \mathbf{S} matrix when solving the prior hydrodynamic system. We describe here the calculus of one representer associated with a data item located at \mathbf{x}_{data} (i.e., indices relative to the observations are omitted). The discrete backward system is written

$$\mathbf{S}^* \eta = \Delta \quad \text{with } \mathbf{S}^* = \begin{bmatrix} 1 & 0 \\ \mathbf{S}_{12}^* & \mathbf{S}_{22}^* \end{bmatrix} \quad \Delta = \begin{bmatrix} 0 \\ \int_{\Omega} \beta_n^* \mu \, ds + \oint_{\partial\Omega_c} \beta_n^* \nu \, dl \end{bmatrix}. \quad (83)$$

Note that the matrix of the adjoint system is not literally the conjugate transpose of \mathbf{S} . In the following, in order to be more explicit, we have to consider two different cases. The first one is where the data are located inside the domain or on the rigid boundary. By definition, the right-hand-side term of the backward problem then becomes

$$\Delta_n = \int_{\Omega} \beta_n^* \mu \, ds + \oint_{\partial\Omega_c} \beta_n^* \nu \, dl = \beta_n(\mathbf{x}_{\text{data}}). \quad (84)$$

It simply represents the value of the interpolation functions β_n at the observation location. We can see here one of the advantages of the variational formulation, which allows us to avoid the problem of discretizing a Dirac function. More generally, using the variational formulation blends naturally with classical measurement formalism. It should be noted that the right-hand-side term is equal to zero, except for the interpolation functions attached to the element nodes, including the observation location. The second case is where the data are located on the open boundary. The right-hand-side term then reduces to

$$\Delta \equiv 0. \quad (85)$$

In this case, the solution for η is zero-valued field. The solution of the forward problem requires us to compute first its boundary conditions. The corresponding discrete system is defined by

$$\mathbf{S} \mathbf{c}_m = \mathbf{\epsilon} \quad \text{with } \mathbf{\epsilon} = \begin{bmatrix} c_o^*(\mathbf{x}_m, \mathbf{x}_n) \\ 0 \end{bmatrix}, \quad (86)$$

where $c_m(\mathbf{x}) = c_{\alpha,\alpha}^*(\mathbf{x}_m, \mathbf{x})$ and m is the index of the boundary node in question. As it does not depend on the data location or value, this system can be solved once and for all before

computing the entire set of representers. Once this system has been solved, the next step is to compute the representer itself. The discrete system is

$$\mathbf{S}r = \mathbf{V} \quad \text{where } \mathbf{V} = \left[\begin{array}{c} c_{\alpha,\alpha}(\mathbf{x}_m, \mathbf{x}_{\text{data}}) \\ \int_{\Omega} \beta_m^* C_i[\eta] ds + \frac{1}{\kappa^2} \int_{\partial\Omega_c} \beta_m^* C_c[\eta] dl \end{array} \right]. \quad (87)$$

4.3. Additional Notes on the Discrete Problem

As it has been brought to our attention, it is interesting to mention an alternative system which solution is identical to the above-developed one (Section 4.2). Let us define the \mathbf{L} vector so that

$$\mathbf{L} = \left[\begin{array}{c} L^*[\beta_1] \\ \vdots \\ L^*[\beta_n] \\ \vdots \\ L^*[\beta_N] \end{array} \right]. \quad (88)$$

Let us define the real symmetric (hence hermitian) B' matrix so that

$$B'_{n,l} = \frac{1}{\kappa^2} \int_{\partial\Omega} \beta_n(\mathbf{x}) \beta_l(\mathbf{x}) ds. \quad (89)$$

The following system, which would be the system to be solved if considering the assimilation in the discrete space from start (i.e., data assimilation in a discrete model), is exactly equivalent, for any type of linear observation functional, to the one derived in Section 4.2:

$$\begin{bmatrix} 1 & \mathbf{S}_{2,1}^* \\ 0 & \mathbf{S}_{2,2}^* \end{bmatrix} \times \begin{bmatrix} \eta'_1 \\ \eta'_2 \end{bmatrix} = \mathbf{L} \quad (90)$$

$$\begin{bmatrix} 1 & 0 \\ \mathbf{S}_{2,1} & \mathbf{S}_{2,2} \end{bmatrix} \times \begin{bmatrix} \mathbf{r}_1 \\ \mathbf{r}_2 \end{bmatrix} = \mathbf{C}_F \begin{bmatrix} \eta'_1 \\ \eta'_2 \end{bmatrix}; \quad (91)$$

here

$$\mathbf{C}_F = \begin{bmatrix} \mathbf{C}_o & 0 \\ 0 & (\mathbf{B}\mathbf{C}_i\mathbf{B} + \mathbf{B}'\mathbf{C}_c\mathbf{B}') \end{bmatrix}.$$

In this case, the matrix of the backward problem is exactly the transpose conjugate of the forward problem. Note that η'_2 is identical to η_2 . The full demonstration would be tedious, but the major points of the derivation are the following:

—the conjugate observation of a discrete field can be expressed as a matrix product

$$\begin{aligned} L^*[\tilde{\alpha}] &= \left(\sum_N \alpha_n \left[\int_{\Omega} \mu^* \beta_n ds + \int_{\partial\Omega_c} v^* \beta_n ds \right] \right)^* \\ &= \sum_N \alpha_n^* \left[\int_{\Omega} \mu \beta_n^* ds + \int_{\partial\Omega_c} v \beta_n^* ds \right] = \tilde{\alpha}^* \times \mathbf{L}; \end{aligned} \quad (92)$$

—due to the interpolation function characteristics, the restriction of L to the inner nodes and rigid limit's nodes is equal to the forcing term of the backward problem:

$$\Delta = \left[\int_{\Omega} \beta_n^* \mu ds + \int_{\partial\Omega_c} \beta_n^* \nu ds \right] = \begin{bmatrix} 0 \\ \mathbf{L}_2 \end{bmatrix}; \quad (93)$$

—the representer boundary condition vector can be expressed as

$$\begin{aligned} \mathbf{r}_o &= [\cdots \mathbf{c}^m \cdots]^* \times \mathbf{L} = \left(\begin{bmatrix} 1 \\ -(\mathbf{S}_{2,2})^{-1} \mathbf{S}_{2,1} \end{bmatrix} \mathbf{C}_o \right)^* \times \mathbf{L} \\ &= \mathbf{C}_o [1 \quad -\mathbf{S}_{2,1}^* (\mathbf{S}_{2,2}^*)^{-1}] \times \mathbf{L}. \end{aligned} \quad (94)$$

This approach avoid the explicit computation of the representer boundary conditions. This is a (very limited) potential gain in terms of computational costs, because we solve (86) by using the impulse responses of the open boundary nodes, computed at a minor cost when solving the prior solution. More interesting is the possibility to reduce the solving procedure. In practice, we solve the linear systems with a direct LU factorization technique. In this approach, the solution of the backward problem could be based on the factorization of the forward system provided some minor manipulations. Nevertheless, the author still favors the approach consisting in developing the assimilation space, then discretizing because it gives a better insight into the assimilation mechanisms. Last but not least, our model is run on a global ocean by computing the solution on separate oceanic basins and removing the boundary condition constraints at the shared limits with a block resolution technique. In this frame, the use of this approach would need further development to compute the global η fields.

5. APPLICATION TO THE SOUTH ATLANTIC M_2 TIDE

The assimilation technique we have just described has been validated and is currently used by the Grenoble group to produce their global solutions. However, the complexity of the full assimilation model does not allow us to give a clear, simple example. We therefore prefer to present an example of the assimilation of tidal gauge data in the Grenoble South Atlantic model, where forcing and rigid boundary conditions have been assumed to be ideal. Thus the only model parameter involved in the general cost function defined in (22) is the term corresponding to the open boundary conditions. There are two motivations for choosing such a test application: first, we know by experience that open boundary conditions are the main sources of error in our model. Second, we deliberately ignore the vast, and complex, problem of quantifying the error covariance of forcing. As mentioned before, the assimilation procedure calls for fairly accurate information on the various errors, and the open boundary condition errors are probably the parameter we are the most comfortable with. Having said that, it must be recalled that this application is an illustration, and does not pretend to be a comprehensive, complete assimilation solution for M_2 . The model design is similar to that used traditionally by the Grenoble group, which is described in previous publications concerning the solution of this model. In short, the spatial resolution is constrained with respect to the local tidal wavelength, and increases from 10 km along the shorelines to a few hundred kilometers in the deep ocean. The bottom topography is derived from ETOPO5 [25] by the optimal technique described in [4]. The loading/self-attraction potential has been deduced from the Texas tidal model CSR3.0 solutions [26] by O. Francis (private communication), using the same technique as in [27]. The CSR3.0 model is defined on a 0.5×0.5 degree grid, with an accuracy for the M_2 solution estimated to be about 1.5 cm

in deep ocean. The so-obtained loading/self-attraction potential thus benefits from better spatial resolution and greater accuracy than the 1×1 degree potential computed originally in [27]. The open boundary conditions, prescribed at the three open limits with the North Atlantic Ocean, Indian Ocean, and South Pacific Ocean, have been interpolated from the CSR3.0 model. The friction coefficients are derived by iteratively solving the hydrodynamic model for the M_2 and K_1 elevations simultaneously, then deriving the corresponding velocities, and reinitializing the friction coefficients with the last obtained velocities (see [28] for more details). After 6 iterations, ensuring the convergence of the friction coefficients, the resulting M_2 tidal elevation solution is taken as the prior solution. The model is assumed to be quasi-linear around this solution, i.e., the actual nonlinear consequences when perturbing the solution are neglected. The observations were selected from the International Hydrographic Office databank [29] (coastal data) and from the International Association for the Physical Sciences of the Ocean (IAPSO) databank [30]. The total dataset contains 61 items, located as shown in Fig. 1. The observation error rms has been set to 1 cm for pelagic data, and 10 cm for coastal data, assuming no correlation between observation errors. The rms of open limit condition errors has been set uniformly to 2.5 cm, with covariance decreasing exponentially in space. The decorrelation distance has therefore been set to 500 km. The lack of sophistication in these error descriptions is due not only to our desire to keep this application simple enough, but also to the lack of pertinent information. Examination of

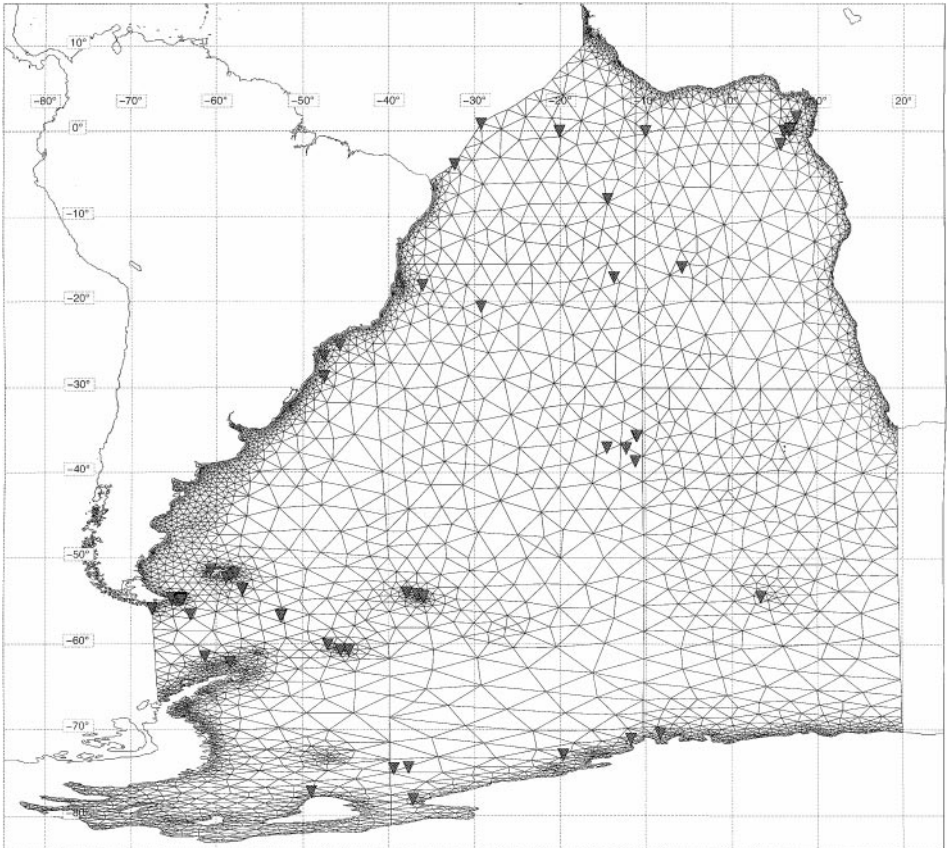


FIG. 1. Model finite-element mesh. Triangles indicate observation locations.

the new solution and its posterior covariance is a means of assessing the quality of the assimilation in a totally internal way. However, as this application is designed to be an illustration, we wish to demonstrate the efficiency of the assimilation. To do so, we need an independent source of information to estimate the gain in accuracy of our solution. In a real case, we strongly recommend using all suitable information in the assimilation itself. The reasons are, first, that the assimilation procedure is the best possible information digester, and, second, it is often the case that there are not enough available data to perform both a good assimilation and to compute significant validation statistics. And if there are, this just means that redundant information is available. The fact is that assimilation is the ultimate validation procedure, and splitting a data set between assimilated data and validation data makes virtually no sense (except of course if the data are of a kind that cannot be used in the assimilation). This point of view might appear extreme, but it is entirely justified when model and observation errors are of a similar range. Because we use most of the available data in the assimilation process, we must rely on a different type of information to compare our assimilated solution. We therefore chose to compare our solutions with the Desai and Wahr (DW) M_2 solution [31]. This is derived from harmonic analysis of the TOPEX/POSEIDON (T/P) altimetric measurements, and therefore is independent of both the data we assimilate and our tidal model, and its accuracy is about 1.5 cm in deep ocean for the M_2 tide. The amplitude of the prior solution is shown in Fig. 2. Because empirical models derived from

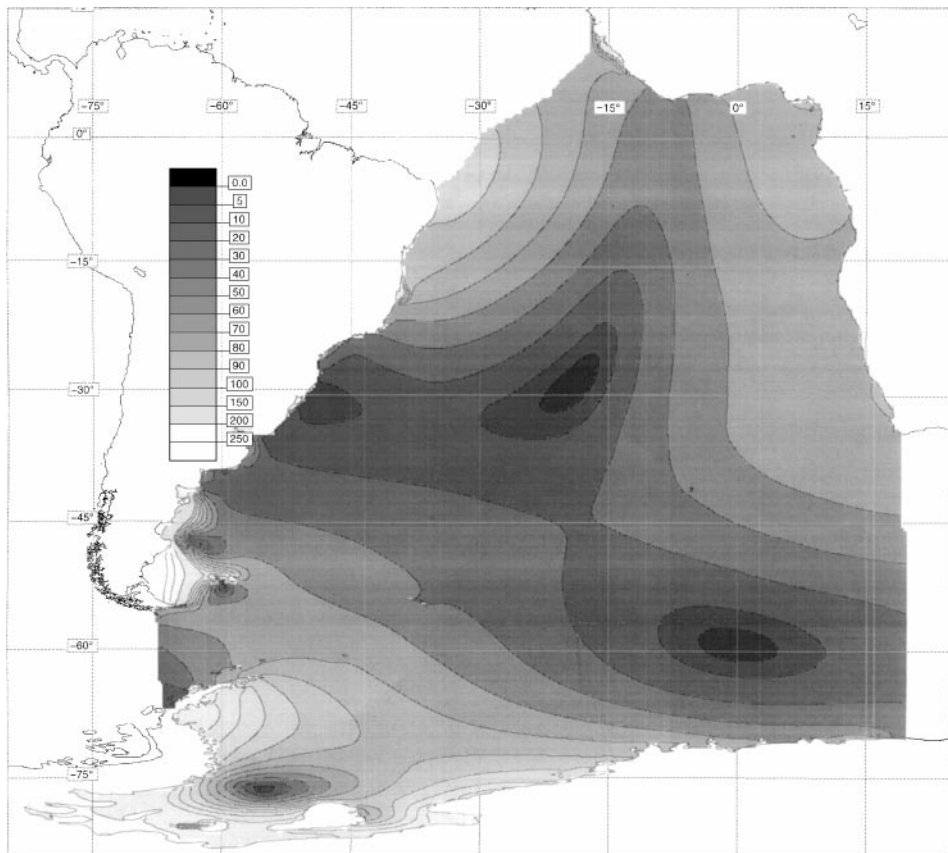


FIG. 2. M_2 tidal amplitude from the model prior solution. Units are in centimeters.

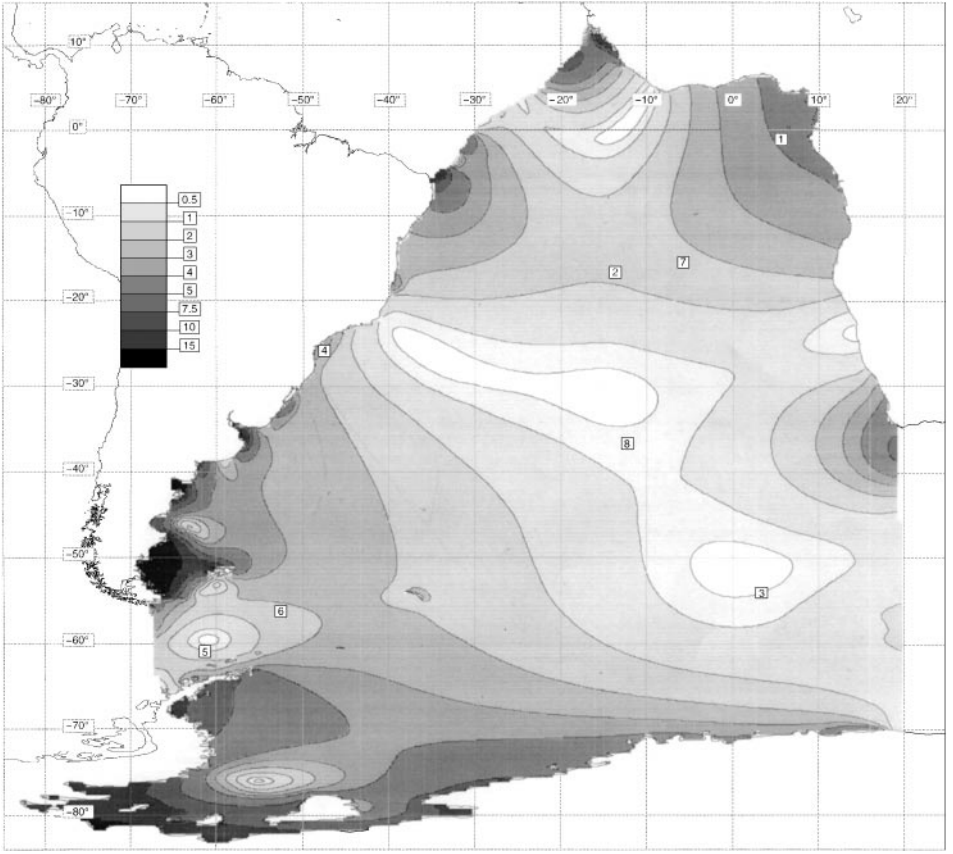


FIG. 3. Modulus of the complex difference between the prior and posterior solutions. Units are in centimeters. Numbers indicate the observation sites listed in Table 1.

T/P are known to be less accurate on shelf areas, we disregard the differences observed on the Patagonian Shelf. The amplitude of the departure of the assimilation solution from the prior one is shown on Fig. 3. The difference between the prior solution and the DW solution, shown in Fig. 4, reveals two main regions, i.e., the Gulf of Guinea and the northern Weddell Sea, where both solutions differ by more than 5 cm, which come from errors of a similar range in our prior solution. The difference between the posterior (assimilated) solution and the DW solution (see Fig. 5) shows a dramatic drop in amplitude, especially in the Gulf of Guinea, which means that the assimilated solution is now much closer to the DW solution, which is an estimate of the sea truth to within 1.5 cm, than the prior solution. Indeed, they are so close in most of the basins that it is nearly within the tidal gauge data observation noise, or error. There are still significant differences in the northern Weddell Sea, which could come from either the DW solution (due to poor satellite coverage during the austral winter) or our solution.

Comparison of the assimilated solution with independent information (the DW model) shows that the results of the assimilation are on the whole satisfactory. In a real application, we should have used the DW model in the assimilation itself as an additional source of observations, so we make the most of the available information we can gather, but leave no independent data to validate the assimilated solution by classical means. We must therefore

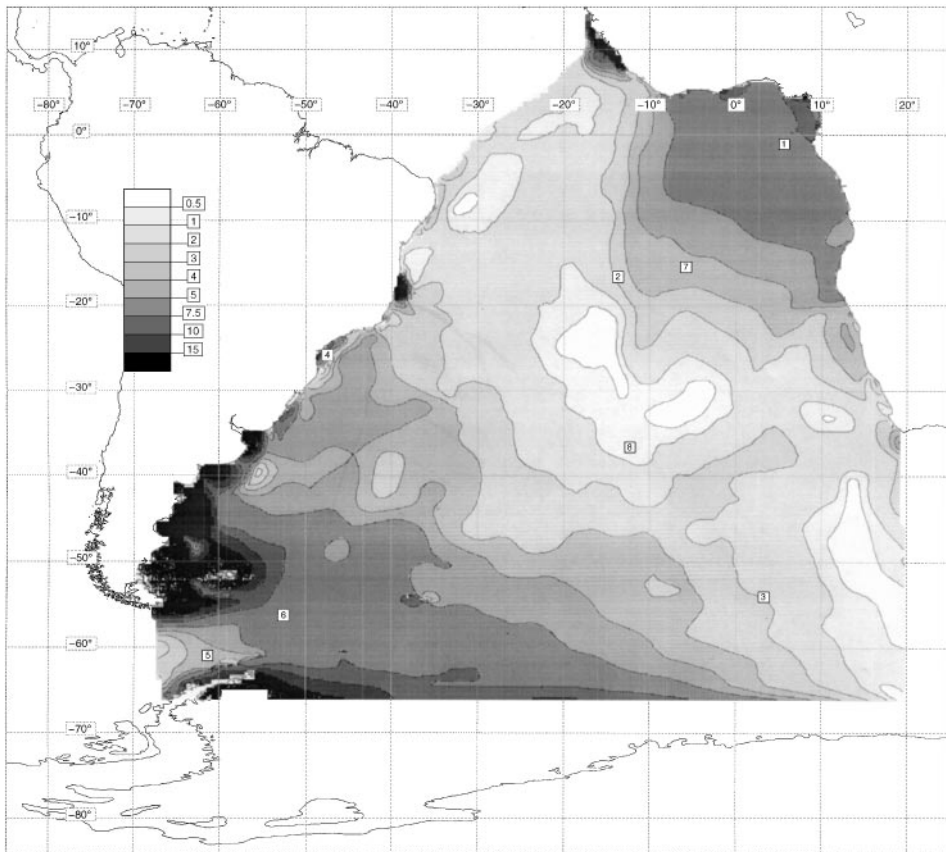


FIG. 4. Modulus of the complex difference between the prior solution and the $M2$ solution given in [31]. Units are in centimeters. Numbers indicate the observation sites listed in Table 1.

rely on internal checks to diagnose the results of the assimilation. This internal validation can be performed by examining first the value of the cost function for the prior model and the assimilated solution. In our application, the former yields 300% and the latter 175%. These numbers represents a departure/noise ratio. For the prior model, the only departure is the data misfit. For the assimilated solution, the departure includes the data misfit plus the departure from the prior model. The first percentage indicates that the prior model is more than significantly different compared to the observations. The comparison between the two ratios also shows that the assimilated solution is a significant improvement over the prior solution. Also, the prior and posterior costs give us an insight into the consistency in the prior error covariance setting. For instance, the prior cost should be greater than 100%, and ideally the posterior cost should approach 100%. One could easily admit that a cost lower than 100% would be physically insignificant (the computed departure would be smaller than the noise level). This 100% limit also has a statistical justification, which is, in short, that the cost function should show a chi-squared random variable behavior. One interpretation of this property is that a set of assimilations, performed by using different data, should lead to a normalized mean cost function equal or close to the number of data, i.e., a 100% ratio. In our example, we probably underestimate the model errors and/or overestimate the data errors.

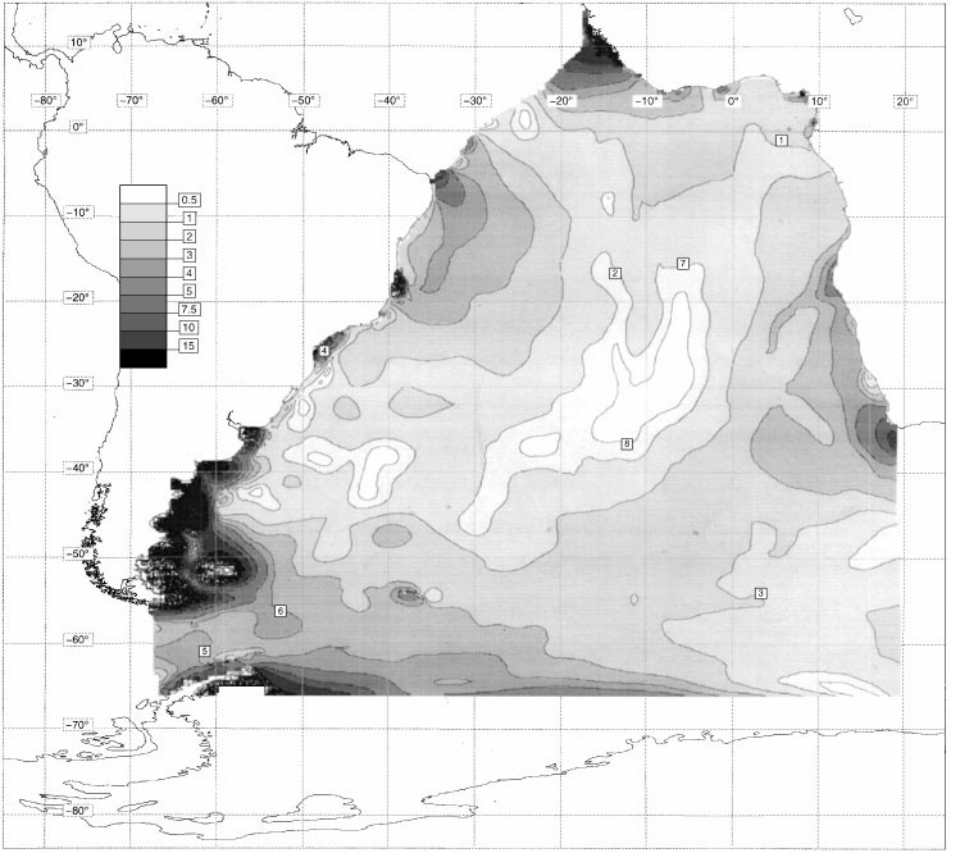


FIG. 5. Modulus of the complex difference between the posterior solution and the $M2$ solution given in [31]. Units are in centimeters. Numbers indicate the observation sites listed in Table 1.

We can also take a closer look at what is going on at each observation site. It is not the aim of this section to give a full analysis, so we have selected a small subset of typical examples, the locations of which are indicated in Figs. 3 and 4. The amplitude, phase, and rms (square root of the variance) of the observations, prior model and posterior model are given in Table 1. First, we wish to check our observation and prior model covariance choices. The prior model variances are the consequence of the error covariance associated with the open boundary conditions. They mainly show an attenuation of the propagated error, except at site #4. The prior model and observation variances are of a similar order, which roughly indicates that, if our description of the model error sources is correct, the prior model is nearly as accurate as the observations. The larger prior model variances appear at sites #5, #6, and #1, and confirm the previously suspected inaccuracy of the prior solution in the Gulf of Guinea and the northern Weddell Sea. In contrast, the prior model variances are less than 1 cm at sites #2, #3, and #8, where our prior solution is very close to the DW solution. Comparing the observation and prior model variances on the one hand, and the computed difference between both on the other, the numbers are once again very consistent, except at sites #1 and #6, where the misfit between observations and prior model is much higher than might be expected if considering the variances. Once again, this occurs where we suspect the prior model to be effectively inaccurate. The observed inconsistency might be an indication that

TABLE 1
Amplitude (A), Phase Lag (g), Confidence (rms) of the Observations,
Prior Model and Assimilation Solution

	A	g	rms	A	g	rms	Δ	A	g	rms
1	50.0	94	1.0	55.5	96	2.2	5.5	50.3	95	1.0
2	16.0	137	1.0	17.0	134	0.5	1.4	15.0	136	0.1
3	14.5	21	0.5	13.0	22	1.0	1.4	13.5	20	0.3
4	24.5	157	1.0	23.0	168	5.0	4.7	26.0	163	2.3
5	32.5	268	1.0	35.5	273	2.5	4.3	35.5	271	2.9
6	40.0	274	1.0	43.5	268	1.6	5.8	41.0	297	0.9
7	32.0	80	1.0	34.0	80	0.8	2.2	31.5	78	0.4
8	22.0	15	1.0	23.5	9	0.6	2.6	23.0	11	0.3

Note. Amplitudes in cm; phases in degrees; rms in cm. Δ is the modulus of the complex difference between observation and prior model elevations.

either the open boundary conditions covariances are not good enough, or that the mode error has a different cause. The variances of the posterior solution also provide useful information. The posterior variances are of smaller range than the prior observations and model variances except at site #5, which indicates good overall consistency of our arbitrary choices. The indication of less than a few millimeters confidence is, however, to be treated with caution, but it certainly shows that the assimilation improved tidal knowledge locally. As pointed out previously, the posterior model shows a significant difference in relation to the DW model in the north Weddell Sea region. Unfortunately, the two sites which could tell us most about these discrepancies are sites #5 and #6, and examination of the assimilation diagnostic indicates a problem with our prior error description at both sites. As a conclusion for this test, a relatively rough application of the assimilation model gives good, acceptable results, but the prior errors should be more precisely described in order to correct the problems identified by the internal diagnostics. One possible improvement would be to modulate the confidence prescribed at the open boundary limits, as we know that the accuracy of the CSR3.0 solution is not uniform. The second most likely improvement would definitely be to use a nonzero covariance for the forcing errors. However, it is clear that assimilation is a complicated application of a simple theory, and special care should be taken always to associate pertinent error bars with the scientific products on which we base our models and databank.

6. DISCUSSION AND CONCLUSION

We proposed here a complete overview of the coupled hydrodynamic and assimilation tidal model developed by the Grenoble group. The assimilation is based on a general inverse method using an L_2 norm-type cost function, applied to a linearized model. It shows that data assimilation can be performed by using a variational formulation that is fully consistent with the hydrodynamic model. In practice, use of the representer approach in penalty function minimization explicitly reduces the dimension of the assimilation problem and avoids inverting the error covariance matrices, which otherwise is a major limitation. Therefore, it is possible to achieve more realistic data and model error covariance description with this approach. The assimilation is formulated without considering actual model discretization

(until discretization is actually needed for the numerical solution). This allows us to gain a better view of the significance of each step that we take, and, as mentioned above, clearly to identify where and how assimilation can be reduced from an infinite-dimension problem to a finite-dimension one. An equally important point is the variational formulation of the assimilation problem. Not only is it fully consistent with the hydrodynamic model, but it also allows the use of sophisticated mathematical tools and concepts like the Dirac functions and, more generally, is very close to the notions developed for measurement theories. From a practical point of view, we feel much more comfortable dealing with equations that handle integrals of a given physical field instead of point-wise values, the significance of which is never clear. This assimilation model has been validated on real applications, and a simplified illustration has been presented in this paper. More generally, it is currently being used to produce the Grenoble global tidal solutions. Because assimilation techniques are to be used more and more in modern modeling, it seems important to us to insist on the need for a rigorous understanding of the intrinsic assumptions that are to be applied when choosing a particular type of cost function. Equally, interpretation of the assimilation results requires a great deal of caution. In theory, the result of assimilation is the new “truth,” or more precisely the best unbiased estimator of the truth, obtained by combining two independent prior items of information. It seems natural to consider that the difference between the assimilation solution and the prior model solution is an indicator of the prior model’s accuracy. Even though it seems more difficult to admit, the difference between the assimilation solution and the observations, plus the covariance given by the posterior matrix, tells us how accurate the observations that we used are. In some ways, assimilation can be seen as a formalization of the classical validation process. Moreover, when the accuracy of observations and the model are of a similar range, i.e., when the noise level is comparable to the prior difference between the observations and model, the classical validation technique proves to be very difficult to interpret, and only an assimilation technique is able to digest the complete information and summarize it. The quality of the assimilation depends considerably on the quality of the prescribed prior covariance, which in practice proves to be one of the major problems of the assimilation process. If there is accurate knowledge of prior errors, our assimilation will also be able to produce accurate information on posterior errors, which could then be used by any modeler taking our results as an input parameter in his own model. The production and delivery of the error bars attached to a solution is as important as the solution itself. We believe that the need for better documented data, as well as model results, is one of the critical challenges that the modeling community will have to face in the future.

APPENDIX: MODIFICATION OF THE REPRESENTER BOUNDARY CONDITION

Because of the linearity of the hydrodynamic system, we can easily establish a model for the elevation-related error $\delta\alpha = \alpha - \alpha_{true}$ due to the input errors $(\delta\psi, \delta\alpha_o, \delta\Phi)$ of the hydrodynamic tidal model. $\delta\alpha$ is the solution of the system

$$S[\delta\alpha] = \frac{1}{\kappa}(i\omega\delta\alpha + \nabla \cdot \mathbf{M}\nabla\delta\alpha) = \delta\psi \quad (\text{A1})$$

associated with the boundary conditions $\delta\alpha = \delta\alpha_o$ on $\partial\Omega_o$ and $\mathbf{M}\nabla\delta\alpha \cdot \mathbf{n} = \delta\Phi$ on $\partial\Omega_c$. We define the elevation error covariance function throughout the domain, including the domain

boundaries:

$$\forall (\mathbf{x}, \mathbf{x}') \in \bar{\Omega} \times \bar{\Omega}, \quad c_{\alpha,\alpha}(\mathbf{x}, \mathbf{x}') = E(\delta\alpha(\mathbf{x})\delta\alpha^*(\mathbf{x}')). \quad (\text{A2})$$

We note that $c_{\alpha,\alpha}$ and c_o coincide for any $(\mathbf{x}, \mathbf{x}')$ belonging to $\partial\Omega_o \times \partial\Omega_o$. Moreover, for any given \mathbf{x}_o belonging to the open boundary, and considering $c_{\alpha,\alpha}$ as a function of \mathbf{x} , we define $c(\mathbf{x}) = c_{\alpha,\alpha}(\mathbf{x}, \mathbf{x}_o)$.

It can easily be shown that c is the solution of the differential system

$$\forall \mathbf{x} \in \Omega, \quad S[c](\mathbf{x}) = \frac{1}{\kappa}(i\omega c + \nabla \cdot \mathbf{M}\nabla c)(\mathbf{x}) = c_{\psi,\alpha}(\mathbf{x}, \mathbf{x}_o) \quad (\text{A3})$$

associated with the boundary conditions $c(\mathbf{x}) = c_o(\mathbf{x}, \mathbf{x}_o) \forall \mathbf{x} \in \partial\Omega_o$ and $[\mathbf{M}\nabla c](\mathbf{x}) \cdot \mathbf{n}(\mathbf{x}) = c_{\Phi,\alpha} \forall \mathbf{x} \in \partial\Omega_c$, where $c_{\psi,\alpha}(\mathbf{x}, \mathbf{x}') = E(\delta\psi(\mathbf{x})\delta\alpha^*(\mathbf{x}'))$, $c_{\Phi,\alpha}(\mathbf{x}, \mathbf{x}') = E(\delta\Phi(\mathbf{x})\delta\alpha^*(\mathbf{x}'))$. Because \mathbf{x}_o belongs to the open boundary, $c_{\Phi,\alpha}(\mathbf{x}, \mathbf{x}_o)$ and $c_{\psi,\alpha}(\mathbf{x}, \mathbf{x}_o)$ are the covariance between the open boundary condition errors and the closed boundary condition errors, respectively, the forcing errors. But $(\delta\psi, \delta\alpha_o, \delta\Phi)$ have been assumed to be independent random fields. So $c_{\Phi,\alpha}(\mathbf{x}, \mathbf{x}_o)$ and $c_{\psi,\alpha}(\mathbf{x}, \mathbf{x}_o)$ are equal to zero. Thus the system reduces to

$$S[c] = \frac{1}{\kappa}(i\omega c_{\alpha,\alpha} + \nabla \cdot \mathbf{M}\nabla c) = 0 \quad (\text{A4})$$

associated with the boundary conditions $c(\mathbf{x}) = c_o(\mathbf{x}, \mathbf{x}_o) \forall \mathbf{x} \in \partial\Omega_o$ and $\mathbf{M}\nabla c(\mathbf{x}) \cdot \mathbf{n}(\mathbf{x}) = 0 \forall \mathbf{x} \in \partial\Omega_c$. Using this property,

$$\begin{aligned} r(\mathbf{x}_o) &= C_o \left[v + \frac{1}{\kappa} \vec{\eta} \cdot \mathbf{n} \right] (\mathbf{x}_o) = \int_{\partial\Omega_o} c_o(\mathbf{x}_o, \mathbf{x}) \left(v + \frac{1}{\kappa} \vec{\eta} \cdot \mathbf{n} \right) (\mathbf{x}) dl \\ &= \int_{\partial\Omega_o} c^*(\mathbf{x}) v(\mathbf{x}) dl + \frac{1}{\kappa} \int_{\partial\Omega_o} c^*(\mathbf{x}) (\vec{\eta} \cdot \mathbf{n})(\mathbf{x}) dl. \end{aligned} \quad (\text{A5})$$

According to the representer open boundary conditions, we can then transform the second term:

$$\begin{aligned} \int_{\partial\Omega_o} c^*(\mathbf{x}) (\vec{\eta} \cdot \mathbf{n})(\mathbf{x}) dl &= \int_{\partial\Omega} c^*(\mathbf{x}) (\vec{\eta} \cdot \mathbf{n})(\mathbf{x}) dl - \int_{\partial\Omega_c} c^*(\mathbf{x}) (\vec{\eta} \cdot \mathbf{n})(\mathbf{x}) dl \\ &= \int_{\partial\Omega} c^*(\mathbf{x}) (\vec{\eta} \cdot \mathbf{n})(\mathbf{x}) dl + \kappa \int_{\partial\Omega_c} c^*(\mathbf{x}) v(\mathbf{x}) dl. \end{aligned} \quad (\text{A6})$$

We first transform the first term of the right-hand side of (A6). Applying the Green theorem and integrating by parts gives

$$\begin{aligned} \int_{\partial\Omega} c^*(\mathbf{x}) (\vec{\eta} \cdot \mathbf{n})(\mathbf{x}) dl &= \int_{\Omega} \nabla \cdot [c^*(\mathbf{x}) \vec{\eta}(\mathbf{x})] ds \\ &= \int_{\Omega} c^*(\mathbf{x}) \nabla \cdot \vec{\eta}(\mathbf{x}) ds - \int_{\Omega} \nabla c^*(\mathbf{x}) \cdot \vec{\eta}(\mathbf{x}) ds. \end{aligned} \quad (\text{A7})$$

The differential backward equation gives

$$\int_{\partial\Omega} c^*(\mathbf{x}) (\vec{\eta} \cdot \mathbf{n})(\mathbf{x}) dl = \int_{\Omega} c^*(\mathbf{x}) (\kappa\mu + i\omega\eta)(\mathbf{x}) ds - \int_{\Omega} (\nabla c^*(\mathbf{x}) \cdot \vec{\eta})(\mathbf{x}) ds. \quad (\text{A8})$$

We wish to transform the second term of the right-hand side in (A8):

$$\int_{\Omega} \nabla c^*(\mathbf{x}) \cdot \vec{\eta}(\mathbf{x}) ds = \langle \nabla c, \mathbf{M}^* \nabla \eta \rangle = \langle \mathbf{M} \nabla c, \nabla \eta \rangle = \int_{\Omega} (\mathbf{M} \nabla c)^*(\mathbf{x}) \cdot \nabla \eta(\mathbf{x}) ds. \quad (\text{A9})$$

Applying the Green theorem and integrating by parts gives

$$\begin{aligned} \int_{\Omega} \nabla c^*(\mathbf{x}) \cdot \vec{\eta}(\mathbf{x}) ds &= \int_{\Omega} \nabla \cdot (\eta(\mathbf{x}) (\mathbf{M} \nabla c)^*(\mathbf{x})) ds - \int_{\Omega} \eta(\mathbf{x}) \nabla \cdot (\mathbf{M} \nabla c)^*(\mathbf{x}) ds \\ &= \int_{\partial \Omega} \eta(\mathbf{x}) \vec{\mathbf{c}}^*(\mathbf{x}) \cdot \mathbf{n} dl - \int_{\Omega} \eta(\mathbf{x}) \nabla \cdot \vec{\mathbf{c}}(\mathbf{x}) ds, \end{aligned} \quad (\text{A10})$$

where $\vec{\mathbf{c}} = \mathbf{M} \nabla c$. Considering the open boundary conditions on η and the rigid boundary conditions on $c(\mathbf{x})$ we note that

$$\int_{\partial \Omega} \eta(\mathbf{x}) \vec{\mathbf{c}}^*(\mathbf{x}) \cdot \mathbf{n} dl = 0. \quad (\text{A11})$$

Using the differential Eq. (A4) gives

$$\int_{\Omega} \eta(\mathbf{x}) \nabla \cdot \vec{\mathbf{c}}(\mathbf{x}) ds = \int_{\Omega} i \omega \eta(\mathbf{x}) c^*(\mathbf{x}) ds. \quad (\text{A12})$$

Replacing in (A8) gives

$$\begin{aligned} \int_{\partial \Omega} c^*(\mathbf{x}) (\vec{\eta} \cdot \mathbf{n})(\mathbf{x}) dl &= \int_{\Omega} c^*(\mathbf{x}) (\kappa \mu + i \omega \eta)(\mathbf{x}) ds - \int_{\Omega} i \omega \eta(\mathbf{x}) c^*(\mathbf{x}) ds \\ &= \kappa \int_{\Omega} c^*(\mathbf{x}) \mu(\mathbf{x}) ds. \end{aligned} \quad (\text{A13})$$

Replacing in (A6) gives

$$\int_{\partial \Omega_o} c^*(\mathbf{x}) (\vec{\eta} \cdot \mathbf{n})(\mathbf{x}) dl = \kappa \int_{\Omega} c^*(\mathbf{x}) \mu(\mathbf{x}) ds + \kappa \int_{\partial \Omega_c} c^*(\mathbf{x}) \nu(\mathbf{x}) dl. \quad (\text{A14})$$

So finally we obtain the new open boundary condition expression

$$r(\mathbf{x}_o) = \int_{\Omega} c_{\alpha, \alpha}(\mathbf{x}_o, \mathbf{x}) \mu(\mathbf{x}) ds + \int_{\partial \Omega} c_{\alpha, \alpha}(\mathbf{x}_o, \mathbf{x}) \nu(\mathbf{x}) dl = L^*(c). \quad (\text{A15})$$

REFERENCES

1. C. Le Provost and A. Poncet, Finite element method for spectral modelling of tides, *Int. J. Numer. Methods Eng.* **12**, 853 (1978).
2. C. Le Provost, A. Poncet, and G. Rougier, Numerical modelling of the harmonic constituents of the tides—Application to the English Channel, *J. Phys. Oceanogr.* **11**(8), 1124 (1981).
3. P. Vincent and C. Le Provost, Semidiurnal tides in the northeast Atlantic from a finite element model, *J. Geophys. Res.* **93**(C1), 543 (1988).
4. F. Lyard and M. L. Genco, Optimization methods of bathymetry and open boundary conditions in a finite element model of ocean tides, *J. Comput. Phys.* **114**, 234 (1994).
5. C. Le Provost, M. L. Genco, F. Lyard, P. Vincent, and P. Cancelli, Spectroscopy of the World Ocean tides from a hydrodynamic finite element model, *J. Geophys. Res.* **99**(C12), 24,821 (1994).

6. C. Le Provost, F. Lyard, M. L. Genco, and F. Rabilloud, A hydrodynamic ocean tide model improved by assimilation of a satellite altimeter derived data set, *J. Geophys. Res.* **103**(C3), 5513 (1998).
7. L. H. Kantha, Barotropic tides in the global ocean from a nonlinear tidal model assimilating altimetric tides, 1. Model description and results, *J. Geophys. Res.* **100**(C12), 25,283 (1995).
8. L. H. Kantha, C. Tierney, J. W. Lopez, S. D. Desai, M. E. Parke, and L. Drexler, Barotropic tides in the global ocean from a nonlinear tidal model assimilating altimetric tides. 2. Altimetric and geophysical implications, *J. Geophys. Res.* **100**(C12), 25,308 (1995).
9. O. Andersen, Global ocean tides from ERS1 and TOPEX/POSEIDON altimetry, *J. Geophys. Res.* **100**(C12) (1995).
10. A. Tarantolla, *Inverse Problem Theory. Method for Data Fitting and Model Parameter Estimation* (Elsevier, New York, 1987).
11. G. Backus, Bayesian inference in geomagnetism, *Geophys. J. Roy. Astron. Soc.* **92**, 125 (1988).
12. E. W. Schwiderski, Ocean tides. II. A hydrodynamic interpolation model, *Mar. Geod.* **3**, 219 (1980).
13. F. O. Jourdin, O. Francis, P. Vincent, and P. Mazzega, Some results of heterogenous data inversions for ocean tides, *J. Geophys. Res.* **96**, 20,267 (1991).
14. G. D. Egbert and A. F. Bennett, *Data Assimilation Methods for Ocean Tides: Modern Approches to Data Assimilation in Ocean Modelling* (Elsevier, New York, 1996).
15. G. Kievman, Assimilating data into open ocean tidal models, in preparation.
16. F. Jourdin, *Assimilation de mesures Marégraphiques at Altimétriques dans un Modèle Hydrodynamique de Marées Océaniques*, Ph.D. thesis (Université Paul Sabatier, Toulouse, 1992).
17. A. F. Bennett and P. C. McIntosh, Open ocean modelling as an inverse problem, *J. Phys. Oceanogr.* **12**, 1004 (1982).
18. C. Le Provost and A. Poncet, *C. Roy. Acad. Sci. B* **285**, 349 (1977).
19. D. R. Lynch, *Oceans 81*, Vol. 2 (IEEE, New York, 1981), p. 810.
20. G. Wahba and J. Wendelberger, Some new mathematical methods for variational objective analysis using splines and cross validation, *Mon. Weather Rev.* **108**, 1122 (1980).
21. R. L. Parker, L. Shure, and J. A. Hildebrand, The application of inverse theory to seamount magnetism, *Rev. Geophys.* **25**, 17 (1987).
22. A. F. Bennett, Inverse methods for assessing ship-of-opportunity networks and estimating circulation and winds from tropical expendable bathythermograph data, *J. Geophys. Res.* **95**, 16 (1990).
23. A. F. Bennett, *Inverse Methods in Physical Oceanography, Monographs on Mechanics and Applied Mathematics* (Cambridge Univ. Press, New York, 1992).
24. G. D. Egbert, A. F. Bennett, and M. G. G. Foreman, TOPEX/POSEIDON tides estimated using a global inverse model, *J. Geophys. Res.* **99**(C12), 24,821 (1994).
25. National Oceanographic and Atmospheric Administration (NOAA), NOAA NGDC Data Announcement 88-MG-02: Digital Relief of the Surface of the Earth, US Department of Commerce, NOAA, NGDC, Boulder, Colorado, 1992.
26. C. K. Shum, P. L. Woodworth, O. B. Andersen, G. Egbert, O. Francis, C. King, S. Klosko, C. Le Provost, X. Li, J.-M. Molines, M. Parke, R. Ray, M. Schlax, D. Stammer, C. Tierney, P. Vincent, and C. Wunsch, Accuracy assessment of recent ocean tide models, submitted for publication.
27. O. Francis and P. Mazzega, Global charts of ocean tide loading effects, *J. Geophys. Res.* **95**(C7) 11,411 (1990).
28. F. H. Lyard, The tides in the Arctic Ocean from a finite element model, *J. Geophys. Res.* **102**(C7), 15,611 (1997).
29. International Hydrographic Office (IHO), *IHO Tidal Constituant Bank*, Ocean and Aquat. Sci., Dep. of Fish. and Oceans, Ottawa, Ont., Canada, 1979.
30. M. J. Smithson, Pelagic tidal constants. 3. IAPSO Publication Scientifique No. 35. Published by the International Association for the Physical Sciences of the Ocean (IAPSO) of the International Union of Geodesy and Geophysics, 1992.
31. S. D. Desai and J. M. Wahr, Empirical ocean tide models estimated from TOPEX/POSEIDON altimetry, *J. Geophys. Res.* **100**(C12), 25,205 (1995).